

Summer 8-31-2009

Non-foster matching of an RFID antenna

Nedime Pelin Yalcin
New Jersey Institute of Technology

Follow this and additional works at: <https://digitalcommons.njit.edu/theses>



Part of the [Electrical and Electronics Commons](#)

Recommended Citation

Yalcin, Nedime Pelin, "Non-foster matching of an RFID antenna" (2009). *Theses*. 315.
<https://digitalcommons.njit.edu/theses/315>

This Thesis is brought to you for free and open access by the Electronic Theses and Dissertations at Digital Commons @ NJIT. It has been accepted for inclusion in Theses by an authorized administrator of Digital Commons @ NJIT. For more information, please contact digitalcommons@njit.edu.

Copyright Warning & Restrictions

The copyright law of the United States (Title 17, United States Code) governs the making of photocopies or other reproductions of copyrighted material.

Under certain conditions specified in the law, libraries and archives are authorized to furnish a photocopy or other reproduction. One of these specified conditions is that the photocopy or reproduction is not to be “used for any purpose other than private study, scholarship, or research.” If a user makes a request for, or later uses, a photocopy or reproduction for purposes in excess of “fair use” that user may be liable for copyright infringement,

This institution reserves the right to refuse to accept a copying order if, in its judgment, fulfillment of the order would involve violation of copyright law.

Please Note: The author retains the copyright while the New Jersey Institute of Technology reserves the right to distribute this thesis or dissertation

Printing note: If you do not wish to print this page, then select “Pages from: first page # to: last page #” on the print dialog screen

The Van Houten library has removed some of the personal information and all signatures from the approval page and biographical sketches of theses and dissertations in order to protect the identity of NJIT graduates and faculty.

ABSTRACT

NON-FOSTER MATCHING OF AN RFID ANTENNA

by

Nedime Pelin Yalcin

In this thesis, novel designs of radio-frequency identification (RFID) tag antennas with better matching characteristics to achieve extended range for passive tags have been investigated in the ultra-high frequency (UHF) band. A variety of cavity-backed/coupled microstrip dipole antennas in 915 MHz range were considered. Additionally, a negative impedance converter designed to cancel out antenna's input capacitance at resonance frequency and to produce the real antenna input impedance was designed, simulated and implemented for an RFID antenna. Numerical simulations have been carried out using ORCAD software package (Cadence), ADS software package (Agilent) and HFSS software package (ANSYS/ANSOFT Inc). Antennas have been designed, fabricated and tested; and a comparison of simulated and measured results were done. Further work is recommended to tune antennas to lower the return loss at operating frequency, in order to achieve an optimized range for use with passive tags.

NON-FOSTER MATCHING OF AN RFID ANTENNA

by
Nedime Pelin Yalcin

A Thesis
Submitted to the Faculty of
New Jersey Institute of Technology
in Partial Fulfillment of the Requirements for the Degree of
Master of Science in Electrical Engineering

Department of Electrical and Computer Engineering

August 2009

Blank Page

APPROVAL PAGE
NON-FOSTER MATCHING OF AN RFID ANTENNA

Nedime Pelin Yalcin

Dr. Edip Niver, Thesis Advisor /Date
Professor of Electrical and Computer Engineering, NJIT

Dr. Gerald Whitman Committee Member /Date
Professor of Electrical and Computer Engineering, NJIT

Dr. Ali N. Akansu, Committee Member /Date
Professor of Electrical and Computer Engineering, NJIT

Dr. William Carr, Committee Member Date
Professor Emeritus of Electrical and Computer Engineering, NJIT

BIOGRAPHICAL SKETCH

Author: Nedime Pelin Yalcin

Degree: Master of Science

Date: August 2009

Undergraduate and Graduate Education:

- Master of Science in Electrical Engineering,
New Jersey Institute of Technology, Newark, NJ, 2009
- Bachelor of Science in Electrical Engineering,
Blacksea Technical University, Trabzon, Turkey, 2005

Major: Electrical Engineering

To my beloved family, teachers and friends.

ACKNOWLEDGMENT

I would like to express my deepest appreciation to Dr. Edip Niver, who not only served as my research supervisor, providing valuable insight and intuition, but also constantly gave me support, encouragement, and reassurance. Special thanks are given to Dr. Gerald Whitman, Dr. Ali N. Akansu, and Dr. William Carr for actively participating in my committee.

I would like to express my deepest appreciation to Mr. Dimple Bhuva, Delta Circuits Inc., for producing the prototype printed circuit board (PCB)s in its facility.

And I also appreciate the help and friendship of Ph.D student Mohamed Ahmed Salem.

Finally, all my special thanks to my family for their endless support, love and belief in me.

TABLE OF CONTENTS

Chapter	Page
1 INTRODUCTION.....	1
1.1 Radio-Frequency Identification Systems and Applications.....	3
1.1.1 Radio Frequency Identification Systems.....	3
1.1.2 Radio Frequency Identification Applications.....	6
1.2 Passive Tags	7
1.3 Active Tags.....	9
1.4 Importance of the Antenna.....	11
1.5 Impedance Matching Techniques.....	12
1.5.1 BALUN.....	12
1.5.2 Negative Impedance Converter.....	13
1.6 Range Extension	14
2 NEGATIVE IMPEDANCE CONVERTER	16
2.1 Introduction	16
2.2 Non-Foster Matching.....	18
2.3 Two-MOSFET Negative Impedance Converter Model.....	19
3 PROPOSED RFID ANTENNAS	20
3.1 Antenna Model-1	21
3.2 Antenna Model-2	23
3.3 Antenna Model-3	25
3.4 Antenna Model-4	28

TABLE OF CONTENTS
(Continued)

Chapter	Page
4 IMPLEMENTATION AND EXPERIMENTAL RESULTS.....	31
4.1 Antenna Model-1 with and without Integrated NIC	31
4.1.1 Antenna Model-1 without Integrated NIC	31
4.1.2 Antenna Model-1 with Integrated NIC	33
4.2 Antenna Model-2 with and without Integrated NIC	34
4.2.1 Antenna Model-2 without Integrated NIC	34
4.2.2 Antenna Model-2 with Integrated NIC	35
5 CONCLUSIONS	38
APPENDIX A - MOSFET PSPICE MODELS	39
APPENDIX B – CIRCUIT SIMULATION SOFTWARE	40
APPENDIX C – ELECTROMAGNETIC SIMULATION SOFTWARE.....	42
APPENDIX D – PRINTED CIRCUIT BOARD DESIGN SOFTWARE	45
REFERENCES	49

LIST OF FIGURES

Figure	Page
1.1 RFID system with passive Tag.....	4
1.2 Time domain waveforms of an RFID system with a passive tag.....	5
1.3 Passive Tag antenna types: 2-wire Folded Dipole and 3-wire Folded	9
1.4 Components of a Passive Tag.....	9
1.5 Example of an Active Tag.....	11
1.6 Equivalent Circuit for an Electrically Small Antenna.....	13
1.7 Practical current-feedback NIC using a pnp – npn pair.....	14
2.1 Equivalent circuit of an Electrically Small Antenna.....	17
2.2 Two-MOSFET Negative Impedance Converter ADS Model.....	19
3.1 Antenna Model-1.....	21
3.2 HFSS S11 Report for Antenna Model-1.....	21
3.3 HFSS Antenna Impedance Report for Antenna Model-1.....	22
3.4 Radiation Pattern for Antenna Model-1.....	22
3.5 Antenna Model-2.....	23
3.6 HFSS S11 Report for Antenna Model-2.....	24
3.7 HFSS Antenna Impedance Report for Antenna Model-2.....	24
3.8 Radiation Pattern for Antenna Model-2.....	25
3.9 Antenna Model-3.....	26
3.10 HFSS S11 Report for Antenna Model-3.....	26
3.11 HFSS Antenna Impedance Report for Antenna Model-3.....	27

**LIST OF FIGURES
(Continued)**

Figure	Page
3.12 Radiation Pattern for Antenna Model-3.....	27
3.13 Antenna Model-4.....	28
3.14 HFSS S11 Report for Antenna Model-4.....	28
3.15 HFSS Antenna Impedance Report for Antenna Model-4.....	29
3.16 Radiation Pattern for Antenna Model-4.....	29
4.1 Constructed Antenna Model-1.....	32
4.2 Measured Input Reflection Coefficient Response $\log S_{11} $ versus f.....	32
4.3 Constructed Antenna Model-1 with integrated NIC.....	33
4.4 Measured Impedance on Smith Chart.....	33
4.5 Smith Chart of Antenna Model-1 with integrated NIC-Cap(min).....	34
4.6 Smith Chart of Antenna Model-1 with integrated NIC-Cap(max)	34
4.7 Constructed Antenna Model-2.....	35
4.8 Measured Impedance on Smith Chart.....	35
4.9 Constructed Antenna Model-2 with integrated NIC.....	36
4.10 Measured Impedance on Smith Chart.....	36
4.11 Smith Chart of Antenna Model-2 with integrated NIC-Cap(min).....	37
4.12 Smith Chart of Antenna Model-2 with integrated NIC-Cap(max).....	37

CHAPTER 1

INTRODUCTION

Radio Frequency Identification System is invented by Léon Theremin as a spying tool for the Soviet Union which retransmitted incident radio waves with audio information in 1946. Sound waves vibrate a diaphragm which slightly alters the shape of the resonator, which modulates the reflected radio frequency. Even though this device was a passive secret listening device, not an identification tag, it has been attributed as a predecessor to RFID technology. The basics concepts used in RFID has been around since the early 1920s according to one source (although the same source states that modern RFID implemetation have been around just since the late 1960s).

Similar technology, such as the IFF (Identification of Friend or Foe) transponder invented in the United Kingdom in 1939, was routinely used by the allies in World War II to differentiate the aircraft as friend or foe. These transponders are still in use in aircraft industry to this day.

Another early work exploring RFID is the landmark 1948 paper by Harry Stockman, titled “Communication by Means of Reflected Power” (Proceedings of the IRE, pp 1196-1204, October 1948). Stockman predicted that “...considerable research and development work has to be done before the remaining basic problems in reflected-power communication are solved, and before the field of useful applications is explored.”

Mario Cardullo’s U.S. Patent 3,713,148 in 1973 was the first true ancestor of modern RFID; a passive radio transponder with memory. The initial device was passive,

powered by the interrogating signal, and was demonstrated in 1971 to the New York Port Authority and other potential users and consisted of a transponder with 16-bit memory for use as a toll collecting device. The basic Cardullo patent covers the use of RF, sound and light as transmission media. The original business plan presented to investors in 1969 showed potential uses in transportation (automotive vehicle identification, automatic toll system, electronic license plate, electronic manifest, vehicle routing, vehicle performance monitoring), banking (electronic check book, electronic credit card), security (personnel identification, automatic gates, surveillance) and medical (identification, patient history) applications.

A very early demonstration of reflected power (modulated backscatter) RFID tags, both passive and semi-passive, was performed by Steven Depp, Alfred Koelle and Robert Freyman at the Los Alamos National Laboratory in 1973. The portable system operated at 915 MHz and used 12-bit tags. This technique is used by the majority of today's UHF and microwave RFID tags.

The first patent to be associated with the abbreviation RFID was granted to Charles Walton in 1983 U.S. Patent 4,384,288 [1].

A basic RFID system consists of a radio-scanner unit, called a *reader*, and a set of remote transponders, denoted as *tags*. The tag includes an antenna and a microchip transmitter with internal read/write memory. In passive tags, the energy required to drive the microchip comes from the interrogation system itself. A backscattering modulation is achieved when the microchip acts as a switch, to match or mismatch its internal load to the antenna. Radio-frequency identification technology, based on the reader/tag paradigm is finding more and more applications in everyday life. Increased sophistication makes

passive tags to be compatible with wide array of sensors permits novel and inexpensive uses for a vast number of applications including but not limited to medicine, retail and military. Especially, after being introduced its applications in medical and military area, more researchers began to concentrate on individual components of RFID systems to improve their performance characteristics. Although RFID systems have too many design-limiting factors, power effectiveness, memory effectiveness and size-reductions; new configurations with novel features are being introduced almost daily.

Several frequency bands have been standardized for this technology. Low frequency (LF, 125-134 kHz), and high frequency (HF, 13.56 MHz) systems are the most mature and accepted worldwide. They are based on quasi-static magnetic flux coupling among the reader's and tag's coils. Ultra-high frequency (UHF, 815 – 860 MHz) and microwave (MW, 2.4 - 5.8 GHz) systems instead involve electromagnetic interaction among radiating antennas and allow longer communication ranges [2] especially in sensor network type applications.

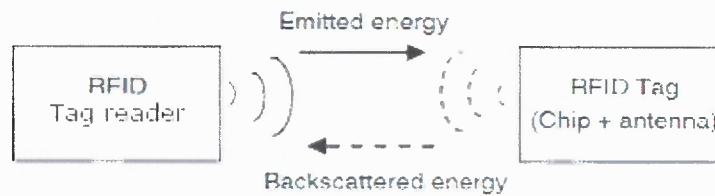
1.1 RFID Systems And Applications

1.1.1 Radio-Frequency Identification Systems

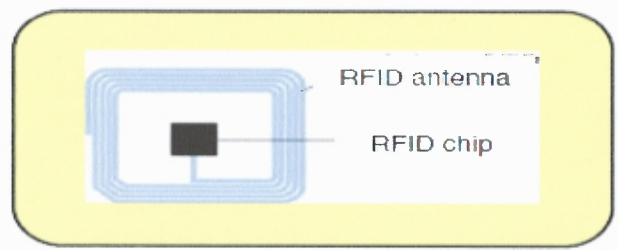
Typically, an RFID system consists of a tag/reader and tag/tags as shown in (Figure 1.1(a)). Tag reader emits interrogating (wake-up) signal which energizes a passive tag, in return tag responds and thus radio frequency identification task of a tag is accomplished. Another attractive alternative is an active tag which can be viewed as a passive tag assisted by a built-in battery. Thus the generic configuration of an active tag consists of an antenna and an integrated circuit chip including the memory. A judicious engineering

design has to include matching the input impedance of the antenna to the output impedance of the chip to ensure the optimum range performance.

A typical passive tag is made up of an antenna and an integrated circuit called chip (Figure 1.1(b)). The chip may contain a detector, rectifying circuit to charge a capacitor for energizing the chip to produce a backscattered signal to an interrogation (wake-up) signal emitted by a tag reader.



(a) Detection principle



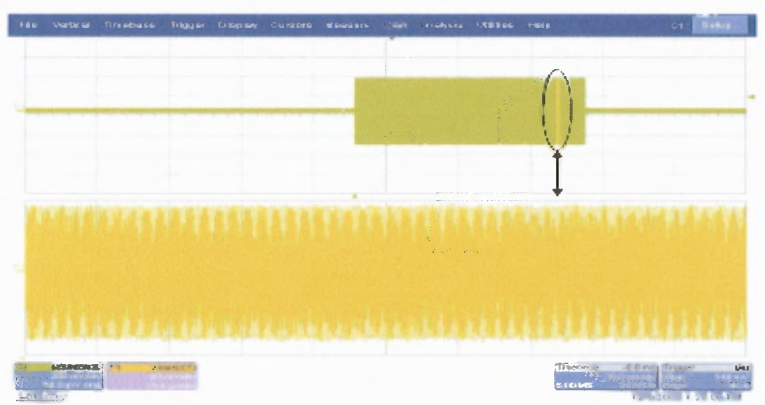
(b) RFID Tag

Figure 1.1 RFID system with passive Tag.

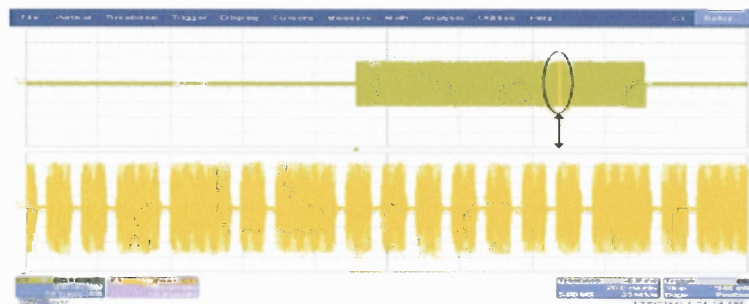
A typical engineering problem is to implement proper matching between the input impedance of the antenna and output impedance of the chip. Proper matching ensures optimum range for the RFID tag operation. A modulated backscattered signal, using for example amplitude shift keying (ASK) modulation, is picked up by the tag reader.

The returned signal usually contains some additional information related to the tag such as an unique serial number or any other information necessary for the identification or the traceability (ex: goods container number, vehicle card number, etc).

Figure 1.2 shows the time domain version of the signal that takes place between the tag reader and the tag in an RFID system. The first figure shows the signal when no tag is present. The second one corresponds to the signal considered at the same moment but in the presence of a tag. By comparing the two waveforms, it can be observed that the tag detection time is longer and the signal level decreases slightly. The detection of the information related to the tag, e.g. its code formed by a sequence of “0” and “1”, is also shown on Figure 1.2(b).



(a) No tag response



(b) One tag response

Figure 1.2 Time domain waveforms of an RFID system with a passive tag.

The maximum distance which permits tag detection is usually called read range. RFID systems can be placed in an environment with multiple signals and interferences.

As a consequence, the read range becomes one of the most important performance measures [3].

1.1.2 Radio-Frequency Identification Applications

The main fields of application for contactless smart cards are payment systems

- Public Transport: Contactless smart cards are widely used as the payment method of transportation fees. This usage makes Automatic Fare Collection (AFC) cheaper, easier and faster, e.g.; EZ-Pass.
- Ticketing: Some airway companies (for example, Lufthansa) issue contactless smart cards to the customers as a replacement of paper-tickets. So, customers can buy tickets using these smart-cards without waiting on the ticket lines. In this way, airline companies can save some labor, also. Another usage of RFID ticketing application is smart ski ticket cards as a replacement of paper ski tickets or passes.
- ID Cards: Access control systems are the most common usage areas of RFID Personal Identification Cards. So that organizations can track the in-out information of customers/members. These cards can be contactless or with contact.Company Pass: Usage of RFID company pass cards gives to employer the opportunity of easy tracking and recording the in-out times, working hours, etc information of each employee.
- Transport Systems: Some railway transportation companies can track each vehicle using RFID vehicle tracking system. In this system, they place an RFID transponder to the bottom face of each vehicle, and an RFID reader on the

railroad at each previously defined checkpoint. Then, whenever a vehicle's tag approaches into the detection zone of a reader, information is retrieved and vehicle's information is sent to the central office immediately. Typical application includes a system called TRANSMIT which is first of its kind to collect real time transportation data using EZ-Pass tags has been installed in New Jersey and New York states [4]

- *Animal Identification:* Stock keeping, carrier pigeon races.
- *Electronic Immobilisation:* Vehicle theft alarm, ignition key.
- *Container Identification:* Gas bottles and chemical containers, waste disposal.
- *Sporting Events:* Runner tracing, winner determination.
- *Industrial Automation:* Tool identification, industrial production.

In the long term we can expect that contactless smart cards will largely replace cards with contacts in their classical fields of application (telephone cards, EC(Eurocard) cards). In addition, contactless technology will allow smart cards to be used in completely new fields – fields may not yet have even thought of [5].

1.2 Passive Tags

This type of RFID tag does not have an on-board power source (for example, a battery), and instead uses the power emitted from the reader to energize itself and transmit its stored data to the reader. A passive tag is simple in its construction and has no moving parts. As a result, such a tag has a long life and is generally resistant to harsh environmental conditions. For example, some passive tags can withstand corrosive

chemicals such as acid, temperatures of 400°F (204°C approximately), and more harsh conditions.

In tag-to-reader communication for this type of tag, a reader always initiates communication by sending a wake-up signal, response followed by the tag reply. The presence of a reader is mandatory for such a tag to transmit its data.

A passive tag is typically smaller than an active or semi-active tag. It has a variety of read ranges starting with less than 1 inch to about 30 feet (9 meters approximately).

A passive tag is also generally cheaper compared to an active or semi-active tag.

A contactless smart card is a special type of passive RFID tag that is widely used today in various areas (for example, as ID badges in security and loyalty cards in retail). The data on this card is read when it is in close proximity to a reader. The card does not need to be physically in contact with the reader.

A passive tag consists of the following main components:

- Microchip: The integrated circuit in the microchip is used for storing and processing information, modulating and demodulating the radio-frequency (RF) signal, and other specialized functions.
- Antenna: A tag's antenna is used for drawing energy from the reader's signal to energize the tag and for sending and receiving data from the reader. This antenna is physically attached to the microchip. The antenna geometry is central to the tag's operations. Various antenna designs are possible, especially for UHF, and designing an effective antenna for a tag becomes as much as an art as a science. The antenna size is directly

proportional to the tag's operating wavelength. Antenna type can be 2-wire folded dipole or 3-wire folded dipole (as shown in Figure 1.3).

Figure 1.4 shows components of a passive tag. [6]

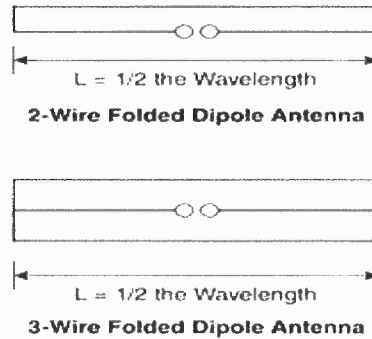


Figure 1.3 Passive tag antenna types: 2-wire folded dipole and 3-wire folded dipole.

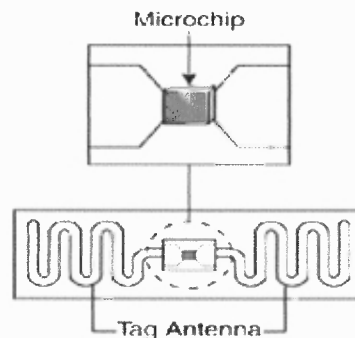


Figure 1-4 Components of a passive tag.

1.3 Active Tags

Active RFID tags have an on-board power source (for example, a battery; other sources of power, such as solar, or thermovoltaic are also possible) and electronics for performing specialized tasks. An active tag uses its on-board power supply to transmit its data to a reader. It does not need the reader's emitted power for data transmission. The on-board electronics can contain microprocessors, sensors. And input/output ports powered by the

on-board power source. Therefore, for example, these components can measure the surrounding temperature and generate the average temperature data. The components can then use this data to determine other parameters such as the expiry date of the attached item. The tag can then transmit this information to a reader (along with its unique identifier). You can think of an active tag as a wireless processor with additional properties (for example, like that of a sensor or a set of sensors).

In tag-to-reader communication for this type of tags, a tag always initiates communication, followed by the response of the reader. Because the presence of a reader is not necessary for data transmission, an active tag can broadcast its data to its surroundings even in the absence of a reader. This type of active tag, which continuously transmits data with or without the presence of a reader, is also called a *transmitter*. Another type of active tag enters a sleep or a low-power state in the absence of interrogation by a reader. A reader wakes up such a tag from its sleep state by issuing a wake-up command. This state saves the battery power, and therefore, a tag of this type generally has a longer life compared to an active transmitter tag. In addition, because the tag transmits only when interrogated, the amount of induced RF noise in its environment is reduced. This type of active tag is called a *transmitter/receiver* (or a *transponder*).

The reading distance of an active tag can be up to 100 feet (30.5 meters approximately) or more when the active transmitter of such a tag is used. An active tag consists of the following main components:

- *Microchip*: The microprocessor size and capabilities are generally greater than the microchips found in passive tags.

- Antenna: This can be in the form of an RF module that can transmit the tag's signals and receive reader's signals in response. For a semi-active tag, this is composed of thin strip(s) of metal such as copper, similar to that of a passive tag.
- On-board power supply
- On-board electronics

Figure 1.5 shows example of an active tag [6].

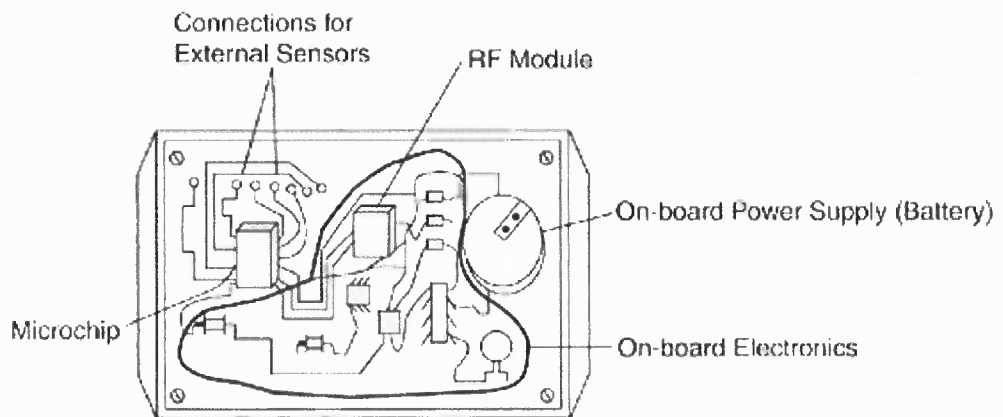


Figure 1.5 Example of an Active Tag

1.4 Importance Of The Antenna

A tag's antenna dimensions are much larger than the tag's microchip, and therefore antenna determines the tag's physical dimensions. An antenna is designed based on several factors, such as the following [6]:

- Operating frequency band
- Tag's reading distance from the reader
- Tag's known orientation to the reader
- Tag's arbitrary orientation to the reader

- Polarization of the reader antenna
- Type of application
- Movement type/speed of the tagged object
- Specific operating/environmental condition(s)
- Reader antenna polarization
- Tag's readability

A mis-tuned antenna makes the tag performance worse; therefore antenna's frequency response should be very carefully considered.

1.5 Impedance Matching Techniques

The basic idea of impedance matching is to match output chip impedance to the input impedance of the antenna to achieve maximum power transfer. Impedance matching is important for the following reasons [7]:

- Maximum power is delivered when the load is matched to the line (assuming the generator is matched), and power loss in the feed line is minimized.
- Impedance matching of sensitive receiver components (antenna, low-noise amplifier, etc.) improves the signal-to-noise ratio of the system.
- Impedance matching in a power distribution network (such as an antenna array feed network) will reduce amplitude and phase errors.

1.5.1 BALUN

Although impedance matching circuits [7] are used in matching source and load impedances, due to size constraints we will only concentrate on baluns only.

Balun is a type of electrical transformer that can convert the impedance of an unbalanced line to a balanced line or vice versa using electromagnetic coupling for its operation.

The most common impedance transformation ratio is 1:4. Baluns having a 1:4 ratio are used between systems with impedances of 50 or 75 ohms (unbalanced) and 200 or 300 ohms (balanced).

In order to operate at optimum efficiency, a balun must be used with loads which are purely resistive.

1.5.2 Negative Impedance Converter

All negative-impedance converters (NIC) use positive feedback to develop a driving-point impedance that is the negative of one of the passive elements used in the feedback loop utilizing active components. If the feedback reference element is a resistor, the resulting two-terminal characteristic is a negative resistance. A negative input capacitance or negative inductance results when we replace the feedback resistor by a capacitor or an inductor.

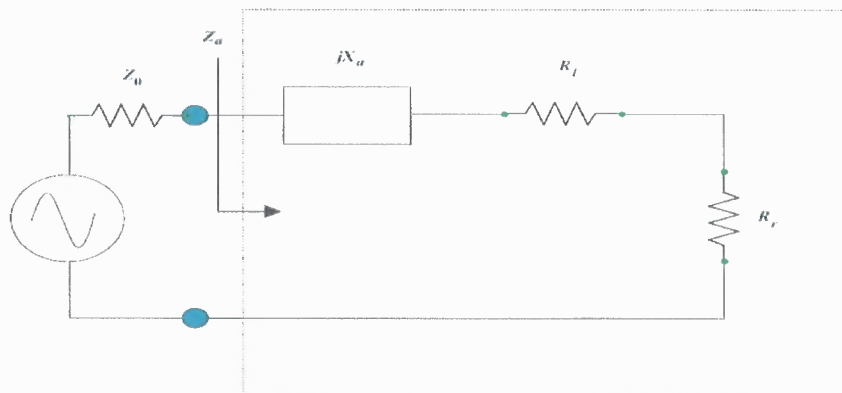


Figure 1.6 Equivalent Circuit for an Electrically Small Antenna [9]

Either a voltage or a current amplifier may be used as the active device. Positive-current feedback creates the current-controlled negative-driving-point impedance, while voltage feedback is used to obtain a voltage-controlled negative impedance.

Figure 1.7 shows a practical current-feedback NIC using a *pnp – npn* pair [4].

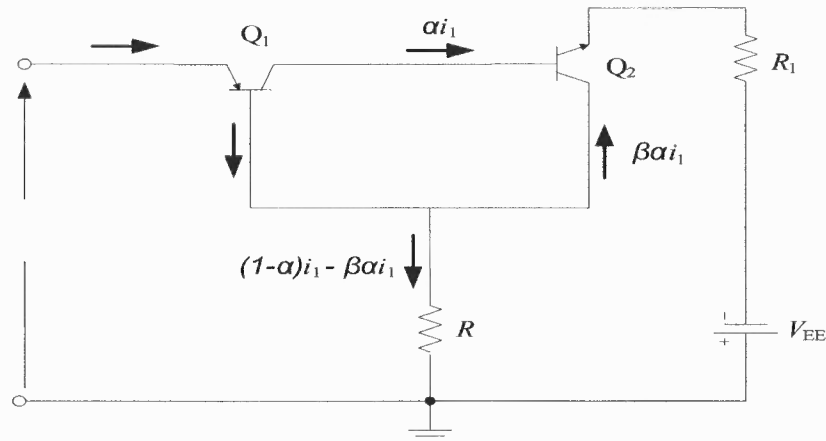


Figure 1.7 Practical current-feedback NIC using a *pnp – npn* pair.

NICs originated in the 1920s as a means to neutralize resistive loss in circuits. According to Merrill, negative impedance circuits were used to develop a new type of telephone repeater called the E1.

Types of NICs can be listed as follows [9]:

- Voltage Inversion NIC (VINIC)
- Current Inversion NIC (CINIC)
- Grounded NIC (GNIC)
- Floating NIC (FNIC)

1.6 Range Extension

When designing for optimum read range, one should primarily consider the reader's power, the tag's power consumption, the tag's quality factor (Q), the tag's tuning, the

reader's antenna aperture, and the tag's antenna aperture. Secondary considerations include the tag's modulation depth, the reader's SNR, the tag's power-conversion efficiency, the reader's antenna tuning and carrier accuracy, the reader's filter quality, how well the reader's driver matches the antenna, the microcontroller's speed and code efficiency, and the tag's data rate.

Sometimes, the modulation type also affects read range. PSK (phase-shift-keying) and FSK (frequency-shift-keying) systems are inherently more immune to noise than ASK (amplitude-shift-keying) systems, because PSK and FSK systems use a subcarrier that noise cannot easily duplicate. In ASK systems, any sufficiently wide noise spike can look like data and corrupt a bit, so you must use checksums, parity schemes, or CRC (cyclic-redundancy checking) to counteract the noise.

The application environment can also affect read range. Key factors include the proximity of the metal surfaces to the tag or reader antennas, the presence of in-band noise sources, whether the tag and reader are stationary or moving, and the angle of the tag with regard to the reader's H-field. Another environmental factor is whether the system is enclosed; a system in a shielded tunnel, for example, can use more power than one in the open air [10].

To increase read range, tag antenna should be designed carefully in order to optimize aperture, Q and tuning parameters of the antenna [8].

CHAPTER 2

NEGATIVE IMPEDANCE CONVERTER

2.1 Introduction

All Negative Impedance Converters (NIC) use positive feedback to develop a driving-point impedance that is the negative of one of the passive elements used in the feedback loop. If the feedback reference element is a resistor, the two-terminal characteristic is a negative resistance. A negative input capacitance or negative inductance results when we replace the feedback resistor by a capacitor or an inductance.

In this thesis negative impedance converter is used to eliminate the reactive component of the input impedance of a tag antenna.

Electrically Small Antennas

An electrically small antenna (ESA) is an antenna whose maximum physical dimension is much less than the free space wavelength λ_0 . One widely accepted definition is that an antenna is considered an ESA at a frequency if it fits inside the so-called *radian sphere*, or

$$k_0 a = \frac{2\pi a}{\lambda_0} < 1$$

where a is the radius of the smallest sphere enclosing the antenna, $k_0 = 2\pi f / c$ is the free-space wave number, and $c \approx 3 \times 10^8$ m/s is the speed of light in vacuum. The input impedance of an antenna can be modeled as a lumped reactance in series with a

radiation resistance. A frequency-domain equivalent circuit for an ESA (or indeed any antenna) is shown in Figure 2.1. Here R_r is the radiation resistance, which represents radiated power delivered by the antenna to its external environment, and R_l represents dissipative losses from the conductors, dielectrics and other materials used to construct the antenna (or present in its immediate environment). For electrically small monopoles and dipoles, the reactance X_a is negative (capacitive), while for electrically small loop antenna X_a is positive (inductive). The antenna impedance in general is given by

$$Z_a = R_r + R_l + jX_a$$

It is a common goal of antenna designers to match this (frequency dependent) impedance to some reference level (often 50Ω) over a given bandwidth with as high efficiency as possible. The exact electrical size of the ESA determines how efficient it can be over a given bandwidth, or equivalently its gain-bandwidth product.

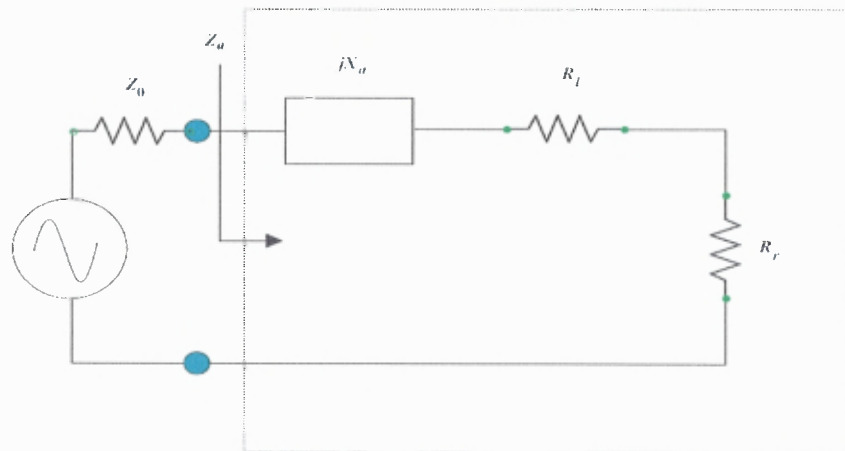


Figure 2.1 Equivalent Circuit of an Electrically Small Antenna

Theoretically, the radiation resistance of an electrically small dipole is given by

$$R_r = 20\pi^2 \left(\frac{l}{\lambda_0}\right)^2 = \frac{20\pi^2}{c^2} l^2 f^2$$

where l is the physical length of the dipole (expressed in meters).

2.2 Non-Foster Matching

The gain-bandwidth limitation of electrically small antennas is a fundamental law of physics that limits the ability of the wireless system engineer to simultaneously reduce the antenna's footprint while increasing its bandwidth and efficiency. The limitations of electrically small antennas imply that high performance on-chip passive antennas can probably never be realized, in spite of the impact of rapidly advancing semiconductor technology on virtually all other aspects of the system. However, it is possible in theory to transform the antenna into an active component that is no longer limited by the gain-bandwidth-size constraints of passive antennas, and whose performance can be improved as semiconductor technology advances. This concept involves the realization of non-Foster reactive components using active circuits called negative impedance converters (NICs). These non-Foster reactances are incorporated into a matching network for the antenna that can cancel out the reactive component of the antenna's impedance and transform the radiation resistance to a reasonable value (like 50Ω) over an octave or more of bandwidth. This revolutionary concept is only beginning to receive attention only in the last decade for antenna applications. Furthermore, present technology limits the maximum frequency of non-Foster reactive components to perhaps a couple of hundred of megahertz at best. However, the potential benefits of this emerging technology are too promising to ignore.

The communication applications where the proposed technology would be most useful (at least initially) are likely to be low data rate, low power, short-distance, unlicensed systems. Initially, this concept is probably not going to be applicable to conventional narrowband transmit applications where active devices in the antenna would

be driven into saturation by the high RF voltages present, resulting in severe distortion of the transmitted signal and concomitant severe interference at many frequencies outside of the device's assigned channel. However, for applications such as ultrawideband (UWB), RFID tags, and sensors where low transmit power is required, the construction of this type of active antenna is likely to be possible for both transmit and receive applications. This innovative approach is the key enabling technology breakthrough required for realization of completely on-chip wireless systems [9].

2.3 Two-Mosfet Negative Impedance Converter Model

In this thesis a Negative Impedance Converter (NIC) circuit, which includes a *pnpn* MOSFET pair as current amplifier, is proposed to match the input impedance of antennas in Chapter 3 which are designed as tag antennas for UHF RFID applications. Figure 2.2 shows an ADS model of a practical implementation of a two-MOSFET NIC used for computer simulation and verification of the NIC's concepts as detailed in [3].

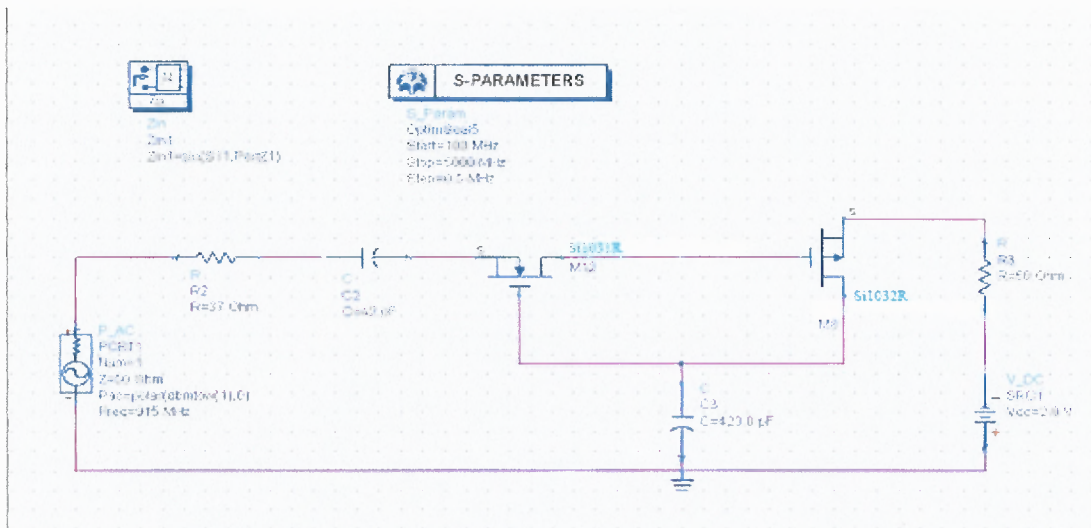


Figure 2.2 Two-MOSFET Negative Impedance Converter ADS Model

CHAPTER 3

PROPOSED RFID ANTENNAS

In this chapter, numerical simulation results and design criteria of proposed antennas will be detailed. The feed structure for the antennas considered in this chapter are solely for possible ease of measurements. In practical tag applications feed can be eliminated or modified when the antenna is directly coupled to the RFID chip output.

All numerical simulations are done using Ansoft HFSS v9.2 Electromagnetic Simulation Software (see Appendix C for a more detailed account on numerical methods for electromagnetic simulation and the software used in thesis).

All antenna models, designed in HFSS v9.2, are configured as a transmitter antenna and fed by a lumped port excitation. As dielectric layer, 30 mils thick FR-4 substrate is used in all models. For conducting parts, copper thickness is selected as 0.1 mil thick.

The central frequency for the RFID tags is chosen at 915 MHz. Sweep is done from 515 MHz to 1.315 GHz for all models. For antenna parameter simulations, the condition of far field radiation is assumed where the field is evaluated on a spherical surface with an infinite radius, radiation patterns were chosen at two azimuthal angles: 0° and 90° and polar angles ranging from -180° to 180° divided in 181 steps.

3.1 Antenna Model-1

Antenna Model-1 is a simple, on-dielectric, ($\lambda/4$) dipole model realized using Marchand-balun with $\lambda/4$ -space between the edges of dielectric and arms of dipole as shown in Figure 3.1. Antenna's resonant frequency is designed at 915 MHz with minimum S_{11} realized at resonance frequency and notch deepness of -10.11 dB as in Figure 3.2.

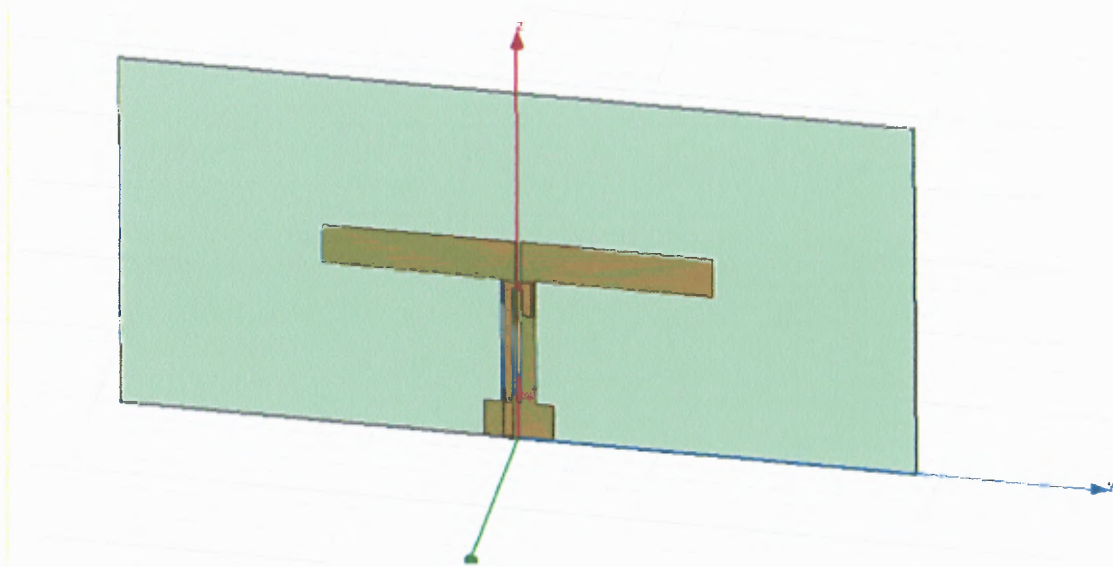


Figure 3.1 Antenna Model-1.

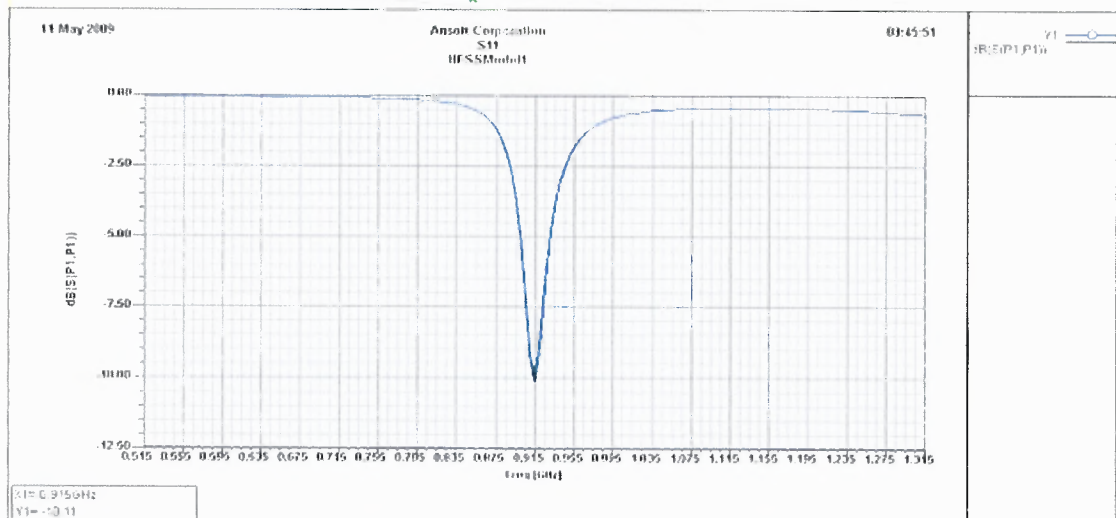


Figure 3-2 The plot of $\log |S_{11}|$ versus the frequency

The antenna impedance at resonance frequency is $(94.24-j*6.94) \Omega$ (cf. Figure 3.3). The radiation pattern of Antenna Model-1 can be seen in Figure 3.4, below:

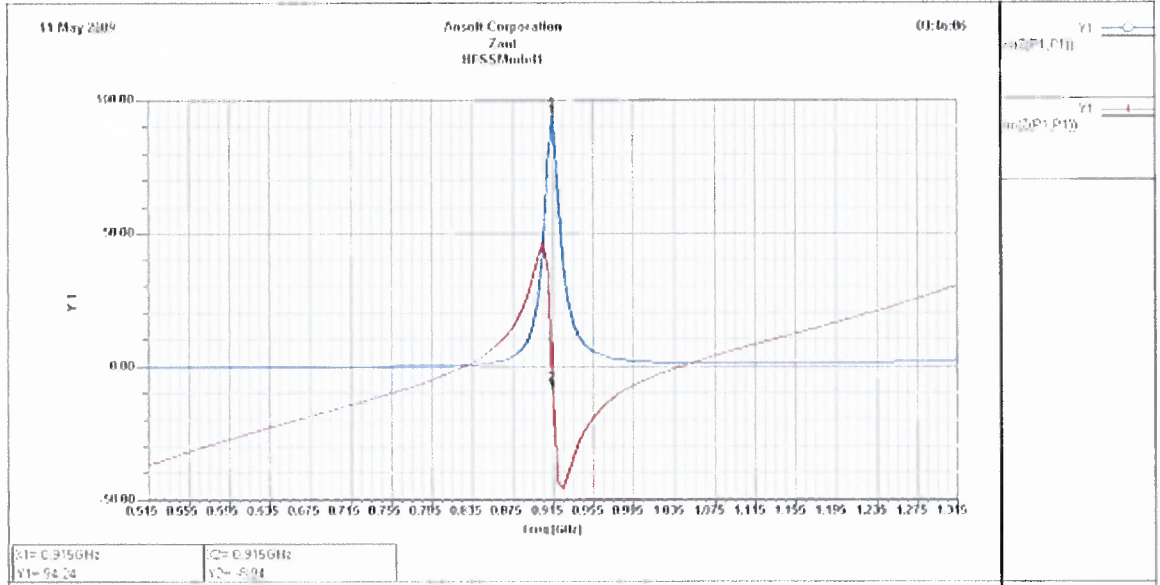


Figure 3.3 HFSS Antenna Impedance Report for Antenna Model-1.

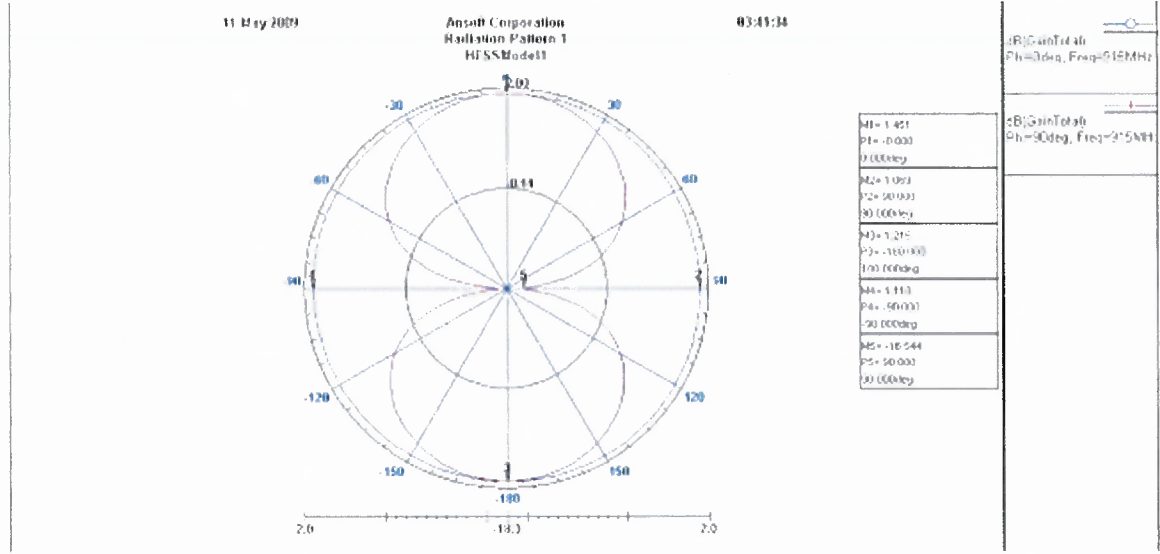


Figure 3-4 Radiation Patterns for Antenna Model-1.

3.2 Antenna Model-2

Antenna Model-2 is the improved version of Antenna Model-1 with coupled two-sided resonator addition. The resonator is supposed to improve the range of the receiving antenna especially compared to the Antenna Model-1. The physical reasoning of the expected improvement is due to excited strong field at the resonator's edge which in turn enhances induced electric field at the dipole end; resulting in stronger current through the feed of the antenna. Resonator fills $\lambda/4$ spaces at each sides of dipole both on the front and back faces of the dielectric substrate. Antenna Model-2 is tuned for 915 MHz resonance frequency. Minimum $\log_{10} |S_{11}|$ is realized at resonance frequency and notch depth is achieved at level of -13.44 dB as shown in Figure 3.6.

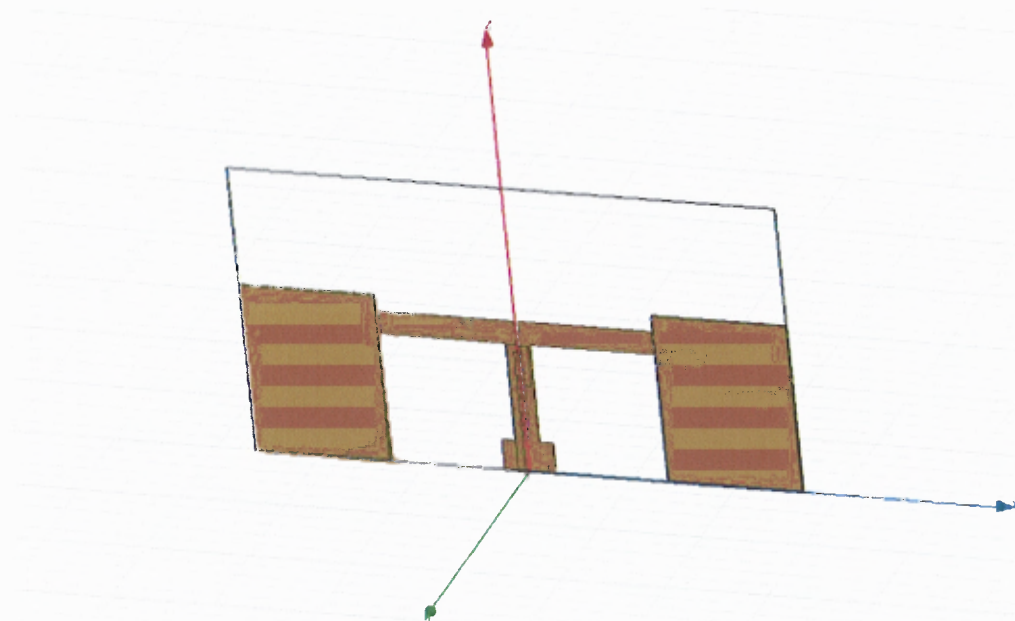


Figure 3.5 Antenna Model-2.

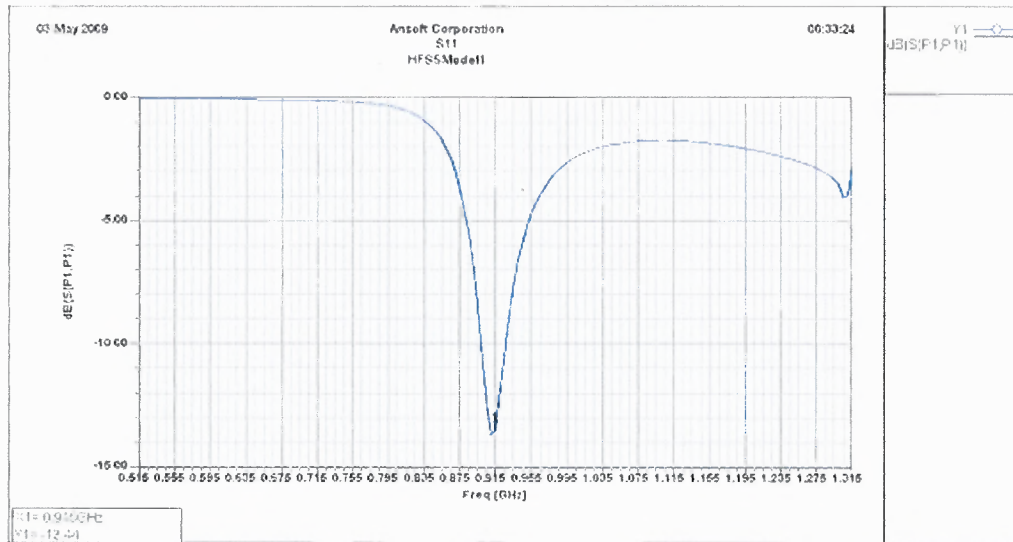


Figure 3.6 The plot of $\log |S_{11}|$ versus the frequency.

Antenna impedance at resonance frequency is $(63.00-j*26.26) \Omega$ (see Figure 3.7).

The radiation pattern of Antenna Model-2 can be seen in Figure 3.8, below:

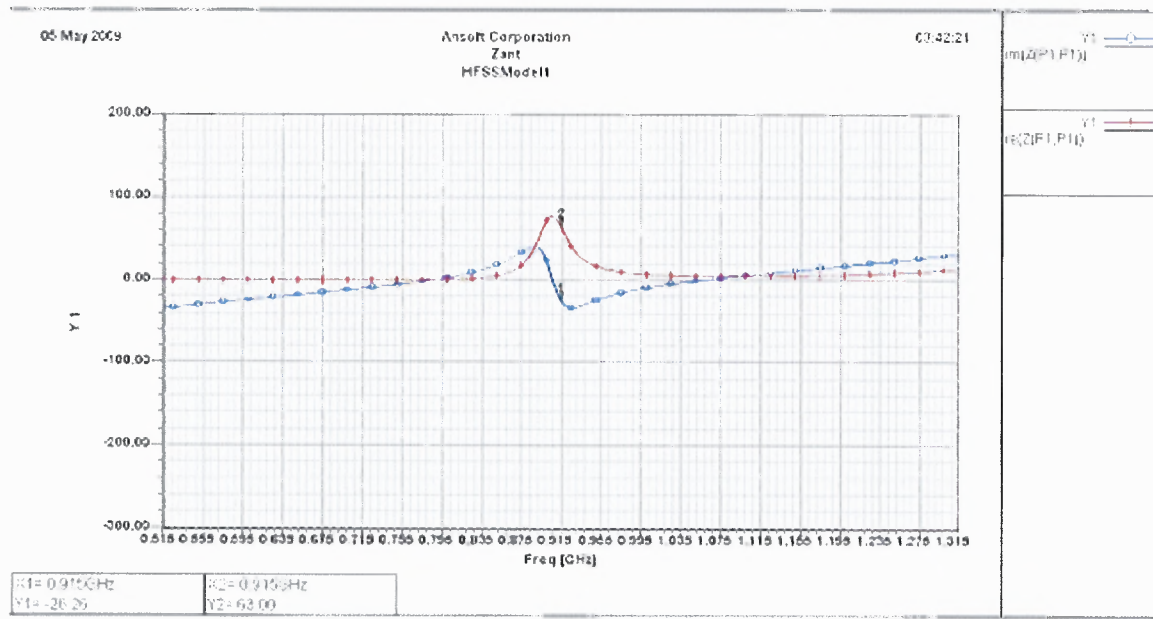


Figure 3.7 Input Antenna Impedance for Antenna Model-2.

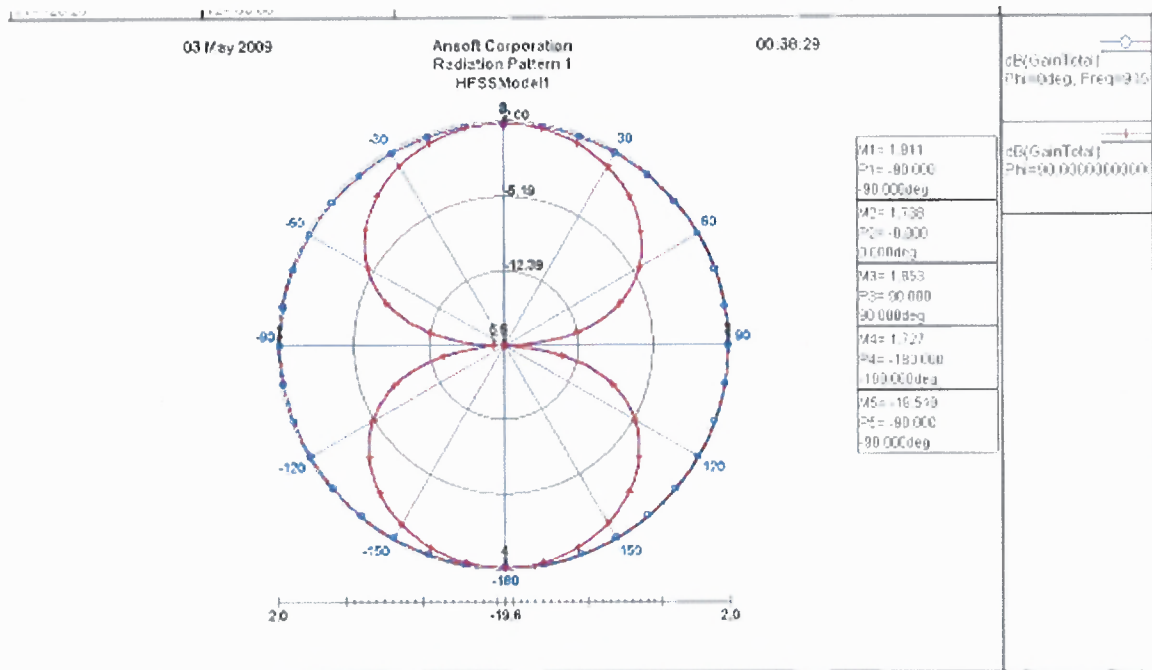


Figure 3.8 Radiation Patterns for Antenna Model-2.

3.3 Antenna Model-3

Antenna Model-3 is the expanded version of Antenna Model-2 with additional air filled back-up cavity, elevated from the ground plane. This modification is supposed to improve the gain by radiating only in the forward direction, thus increasing the range of the antenna comparing to antennas in Model-1 and Model-2 as shown in Figure 3.9. Antenna Model-3 is also tuned for 915 MHz resonance frequency. Minimum $\log |S_{11}|$ is realized at resonance frequency yielded notch depth as -29.26 dB as can be seen in Figure 3.10:

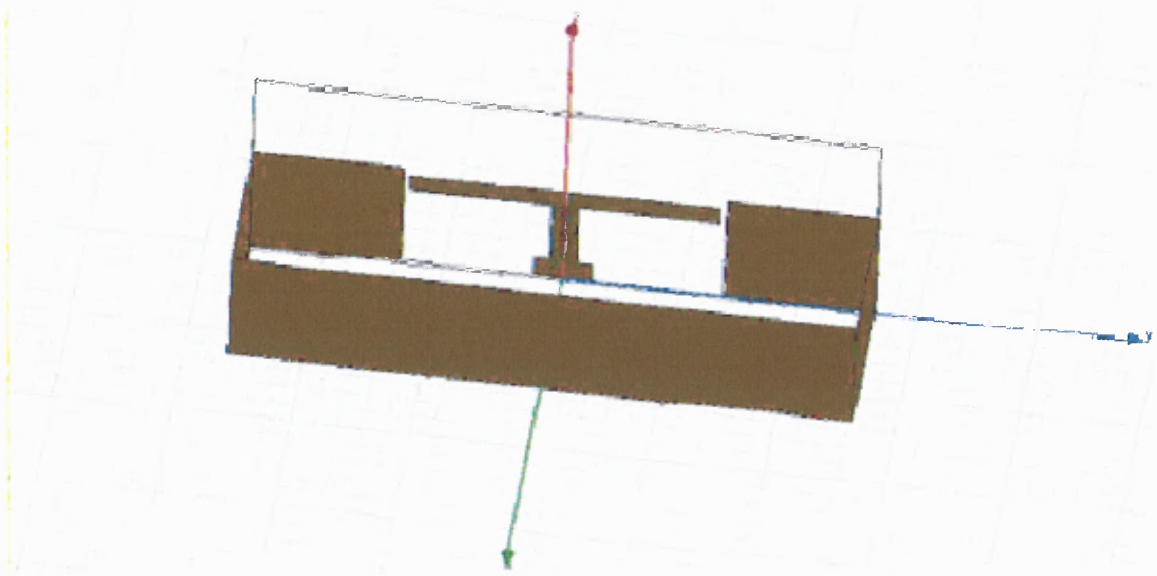


Figure 3.9 Antenna Model-3.

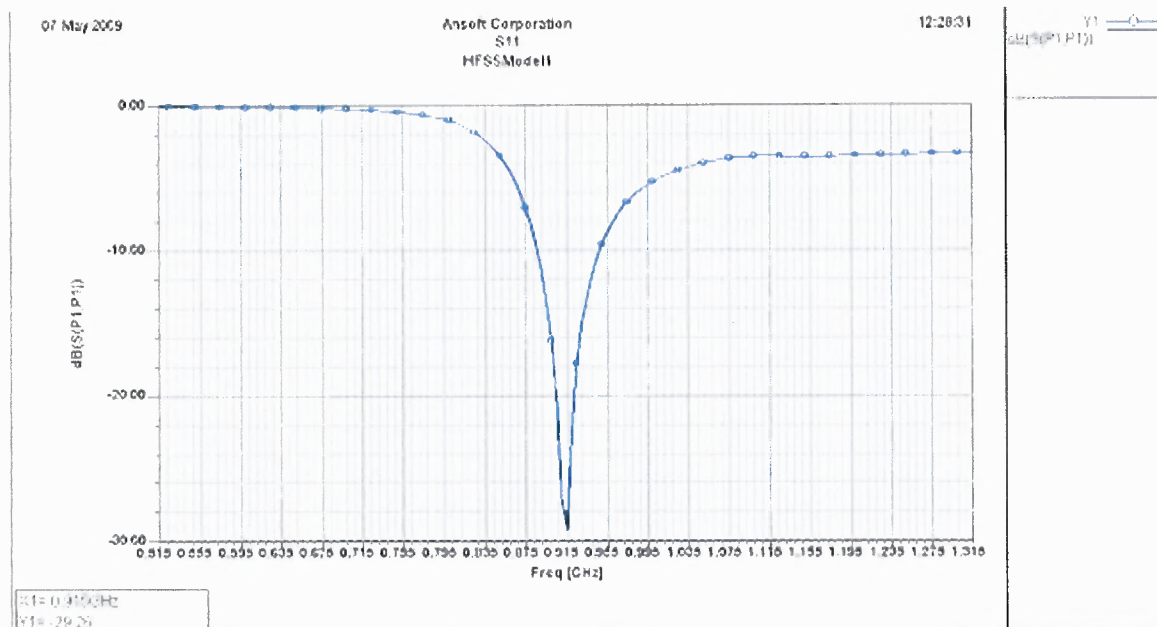


Figure 3.10 The plot of $\log |S_{11}|$ versus the frequency.

Antenna impedance at resonance frequency yielded $(46.94-j1.33) \Omega$ as shown in Figure 3.11. The radiation patterns of Antenna Model-3 are depicted in Figure 3.12:

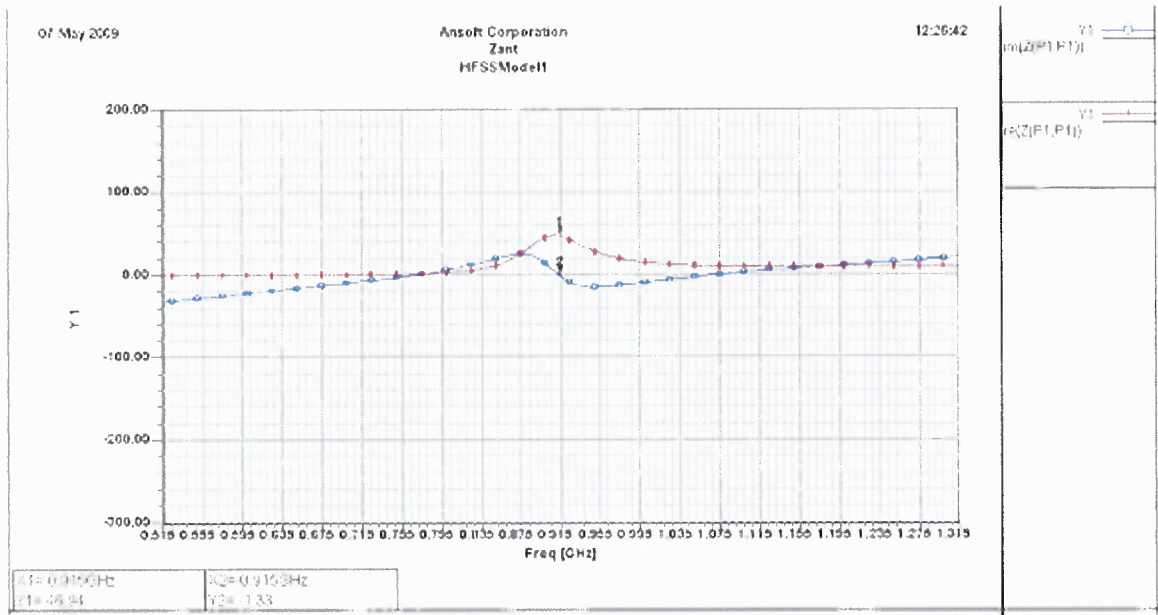


Figure 3.11 HFSS Antenna Impedance Report for Antenna Model-3.

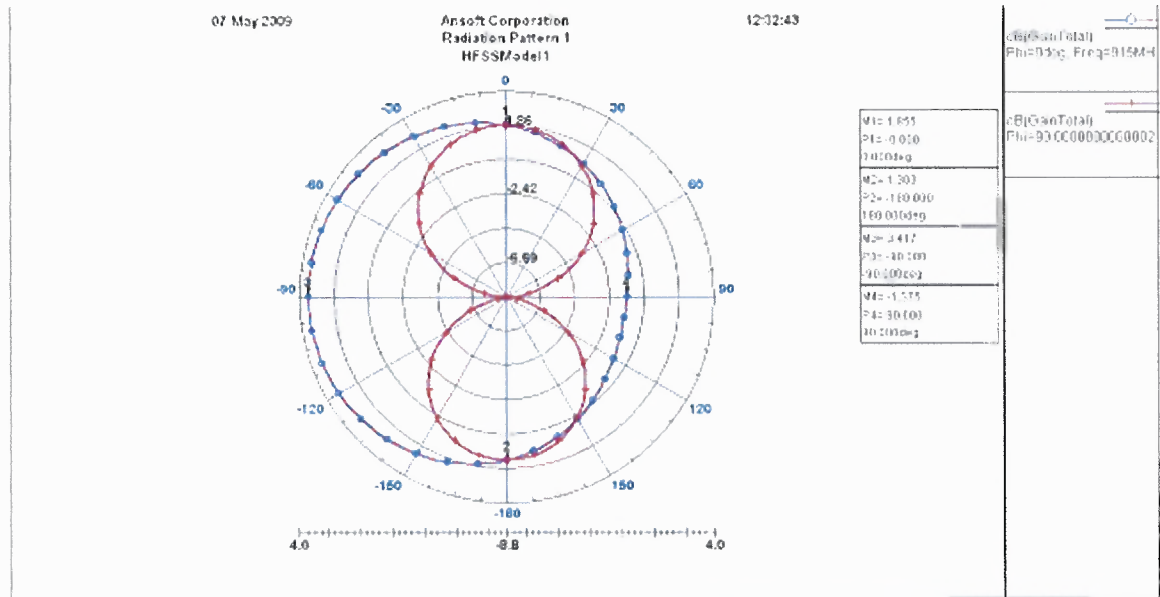


Figure 3.12 Radiation Patterns for Antenna Model-3.

Despite the improvement in gain, this configuration increases overall volume of the antenna significantly due to additional height of the cavity.

3.4 Antenna Model-4

Antenna Model-4 is the compact version of the antenna Model-3 resulting in reduction of the overall volume significantly. Minimum $\log |S_{11}|$ is tuned to the resonance frequency of 915 MHz and notch depth is observed to be at -18.47 dB as can be seen in Figure 3.14 below.

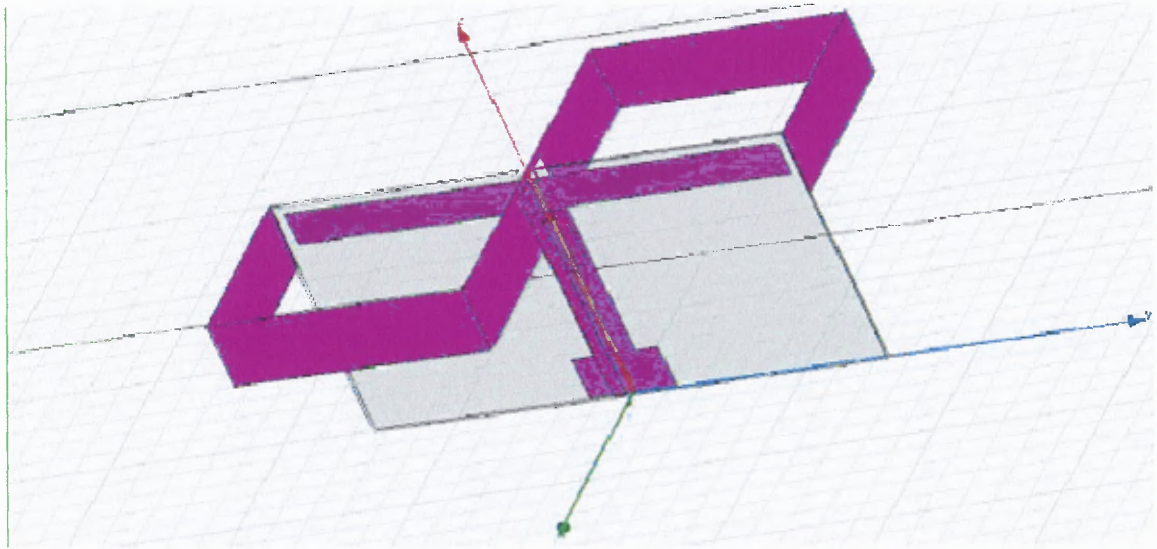


Figure 3.13 Antenna Model-4.

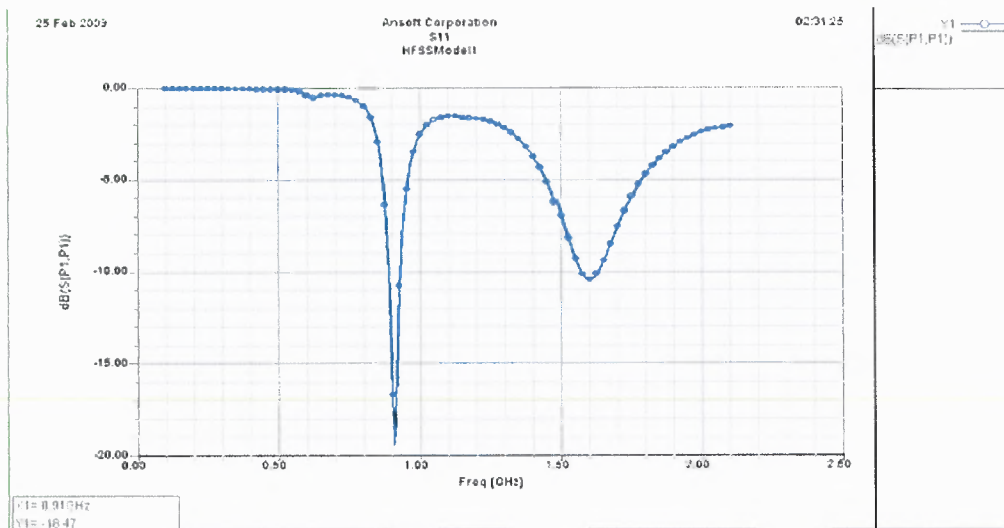


Figure 3.14 The plot of $\log |S_{11}|$ versus the frequency.

Antenna impedance at resonance frequency is observed to be $(58.84-j*9.58) \Omega$ as shown in Figure 3.15. The radiation patterns of Antenna Model-4 are included in Figure 3.16:

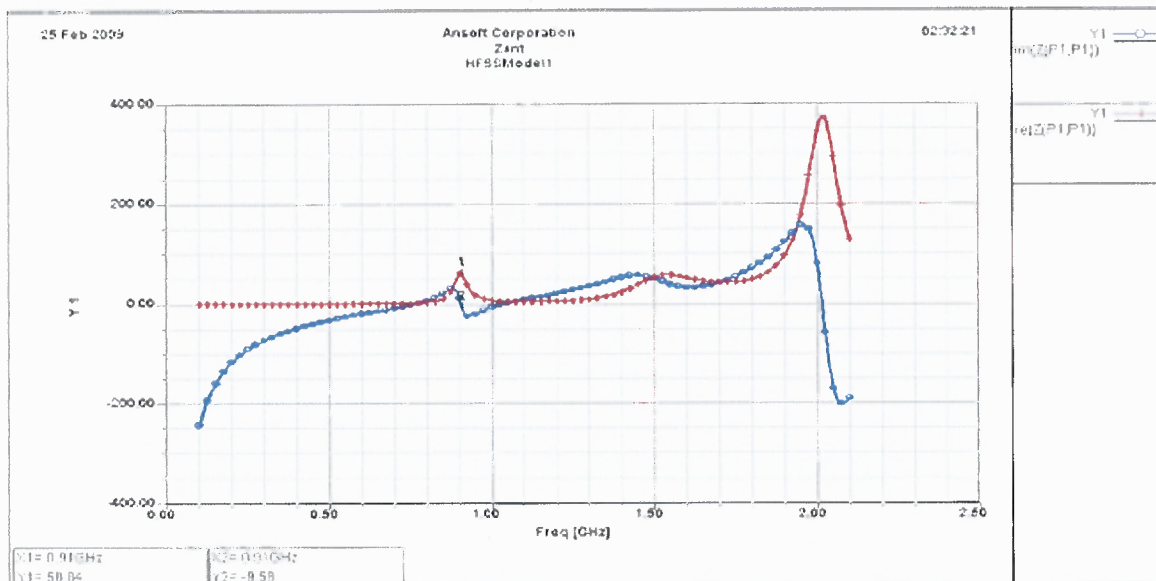


Figure 3.15 Antenna Impedance versus frequency f for Antenna Model-4.

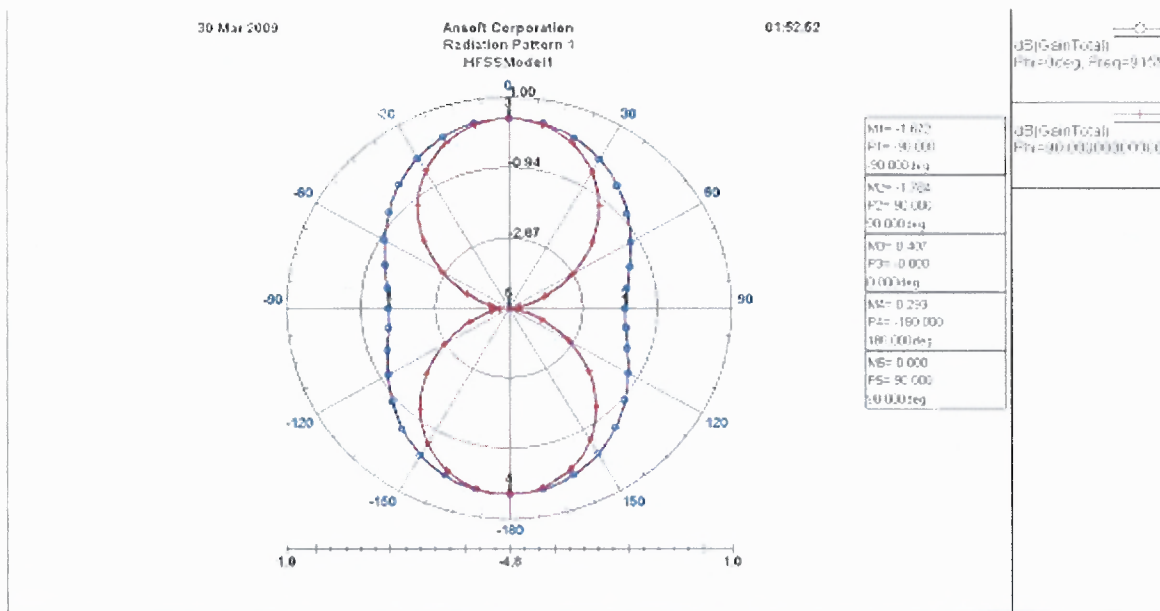


Figure 3.16 Radiation Patterns for Antenna Model-4.

The configuration of Antenna Model-4 is attractive for practical implementation where the dipole antenna can be replaced with electrically short antenna with eliminated feed structure yielding very compact antenna with significant gain and range improvements.

CHAPTER 4

IMPLEMENTATION AND EXPERIMENTAL RESULTS

Antennas simulated in Chapter 3 were constructed on FR4 substrate. After connectorizing the feed structure with SMA connectors, initial response was measured using 8510C Vector Network Analyzer. There was some discrepancies which were attributed to uncertainties of the FR4 substrate's dielectric permittivity and possible errors during the simulations. During measurements for S11- the input reflection coefficient minimal additional tuning in terms of adding metal tape on the dipole arms was carried out to retune the operating frequency to be centered at 915 MHz. Simulation results served as a good benchmark for constructing the antennas. Furthermore, Negative Impedance Converter (NIC) was constructed using variable capacitor as a tuning element. The results of this experimental investigation is outlined below.

For the NIC implementation of Antenna Model-1 Si1031R – Vishay P-Channel 20-V (D-S) MOSFET [19] is used as the input stage transistor (Q1) and Si1032R – Vishay N-Channel 1.5-V (G-S) MOSFET [20] is used as the output stage transistor (Q2). As the capacitor (C1), Johanson MFG Corp Thin-Trim Capacitor Kit JK-942SL, 9402-6SL-1 (6.0 – 25 pF Yellow) is used [21].

4.1 Antenna Model-1 With And Without Integrated Nic

4.1.1 Antenna Model-1 without Integrated NIC

Constructed antenna was measured and after tuning process involving addition of copper tape on dipole's arms, the response was measured at 915 MHz. The depth of the

resonance notch corresponding to $\log |S_{11}|$ observed to be at -30.434 dB. The physical antenna and its measurement results are shown in Figures 4.1 and 4.2.

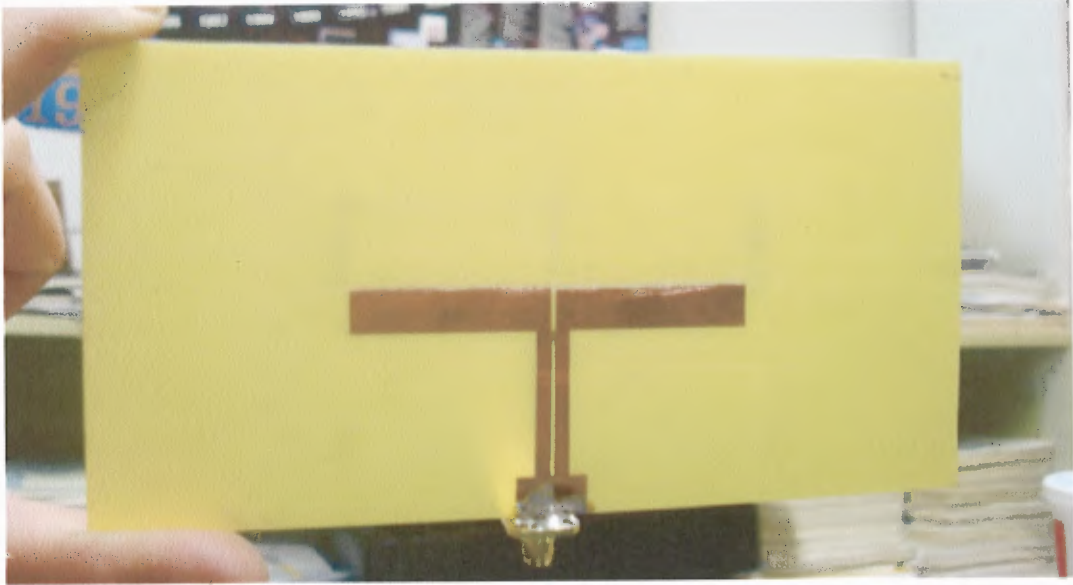


Figure 4.1 Constructed Antenna Model-1

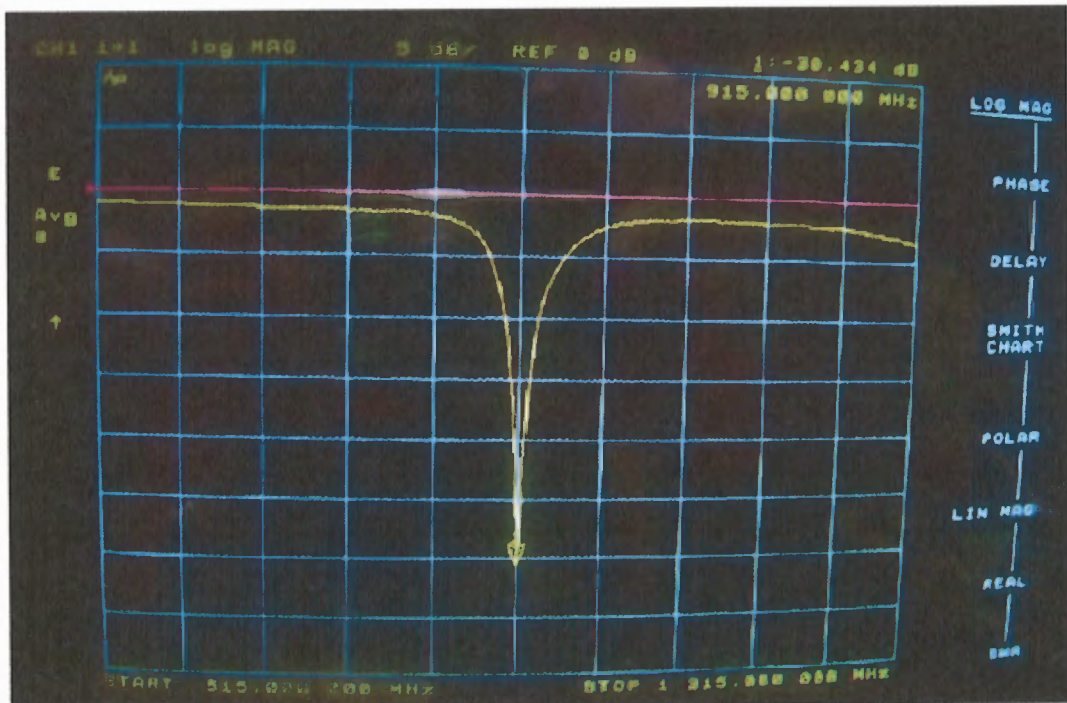


Figure 4.2 Measured Input Reflection Coefficient Response $\log |S_{11}|$ versus f

4.1.2 Antenna Model-1 with Integrated NIC

Figure 4.3 shows the constructed version of the Antenna Model-1 with integrated NIC circuitry. Figure 4.4 depicts the Smith Chart plot for this antenna with the integrated NIC with no V_{SS} voltage applied and Figure 4.5, 4.6 show the measurement results of the same parameter with an applied V_{SS} voltage of $-1.5V$ for, respectively, minimum and maximum values of the tunable capacitor.

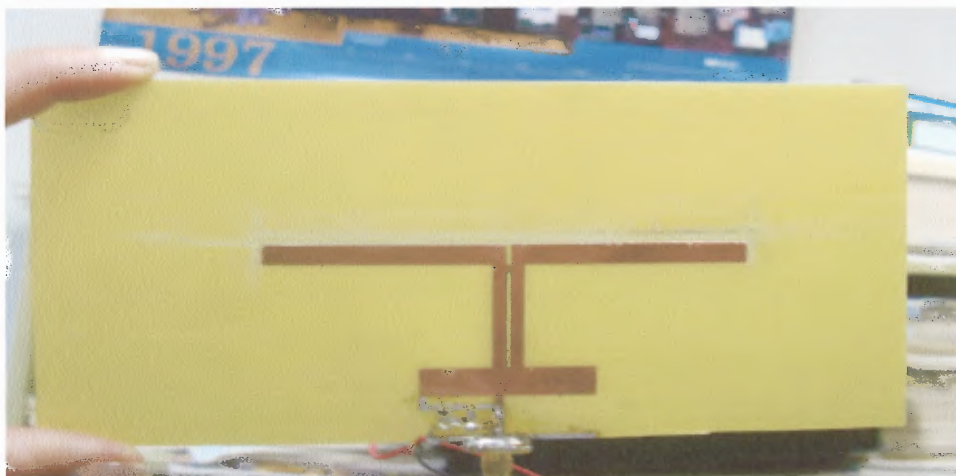


Figure 4.3 Constructed Antenna Model-1 with integrated NIC

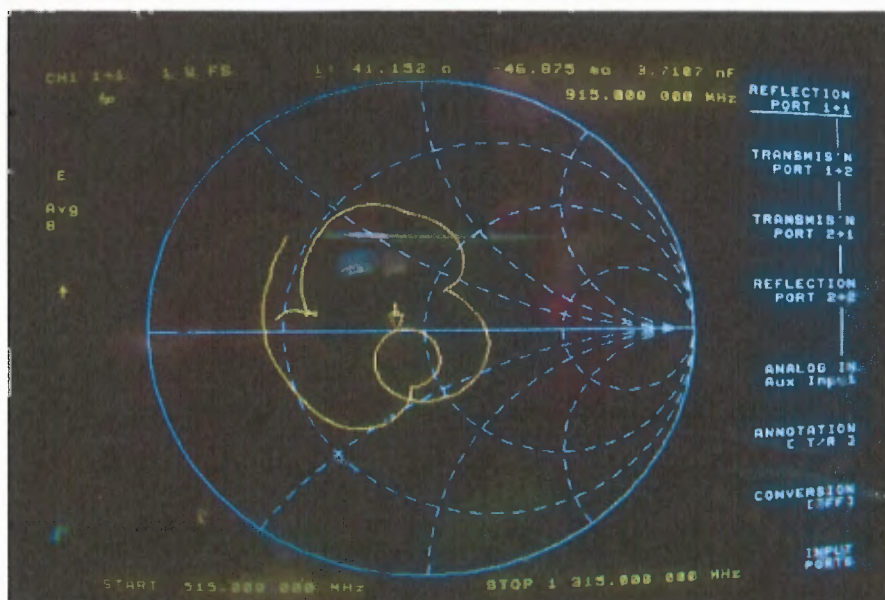


Figure 4.4 Measured Impedance on Smith Chart

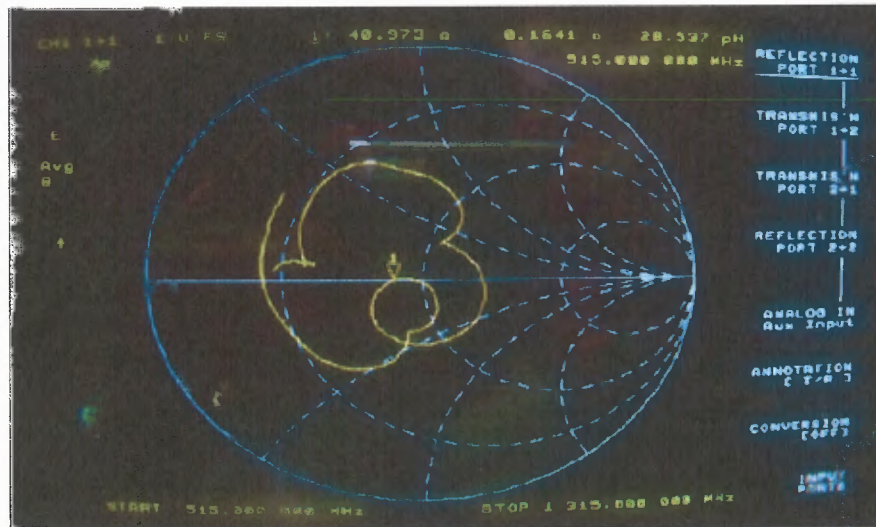


Figure 4.5 Smith Chart of Antenna Model-1 with integrated NIC-Cap(min)

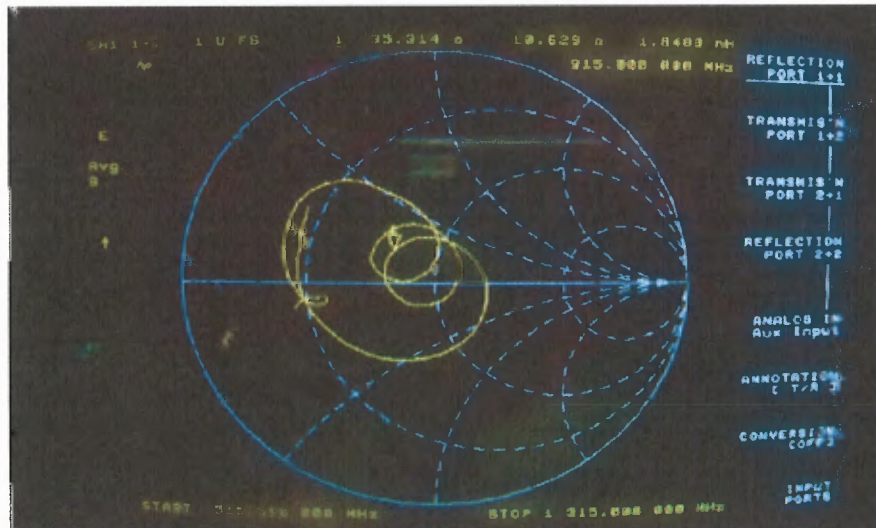


Figure 4.6 Smith Chart of Antenna Model-1 with integrated NIC-Cap(max)

4.2 Antenna Model-2 With And Without Integrated Nic

4.2.1 Antenna Model-2 without Integrated NIC

The constructed antenna was re-tuned using copper tape until the resonance notch occurred at 915 MHz. The input reflection coefficient was measured to be $\log |S_{11}|$

equal to -19.374 dB. The produced antenna board and measurement result are shown in Figures 4.7 and 4.8.

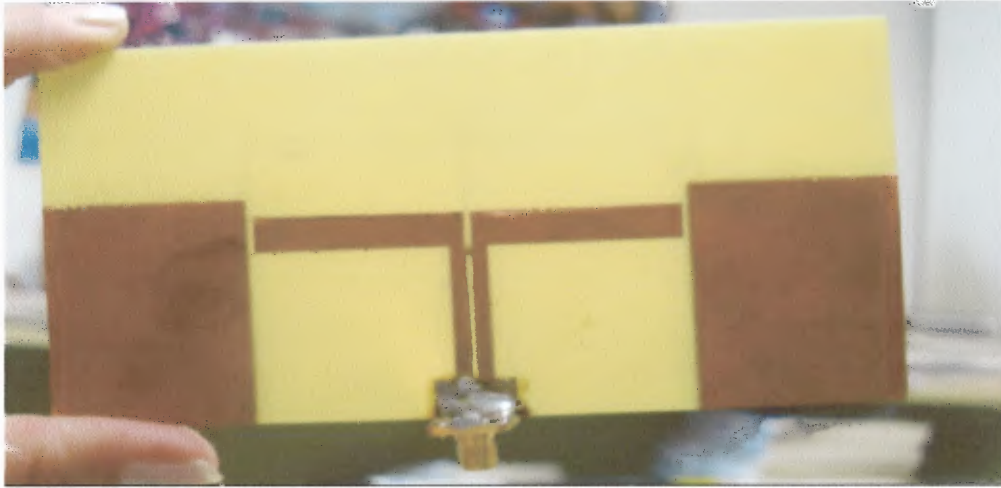


Figure 4.7 Constructed Antenna Model-2 without integrated NIC.

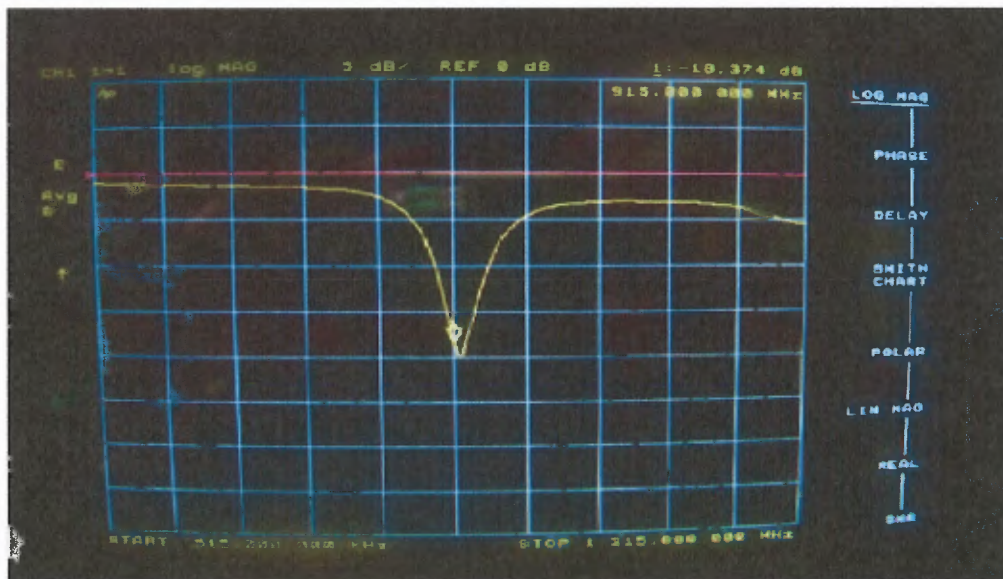


Figure 4.8 Measured Input Reflection Coefficient Response $\log |S_{11}|$ versus f

4.2.2 Antenna Model-2 with Integrated NIC

Figure 4.9 shows the constructed Antenna Model-2 with integrated NIC circuitry. Figure 4.10 depicts the measured input reflection coefficient $\log |S_{11}|$ versus frequency with

the integrated NIC with no V_{ss} voltage applied as well measured data with applied V_{ss} voltage of -1.5V for different values of the tunable capacitor.

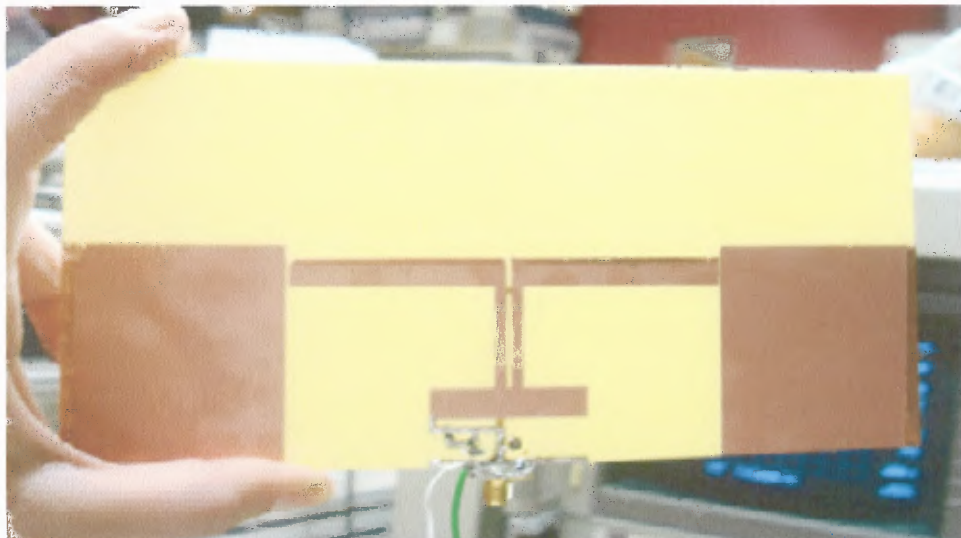


Figure 4.9 Constructed Antenna Model-2 with integrated NIC

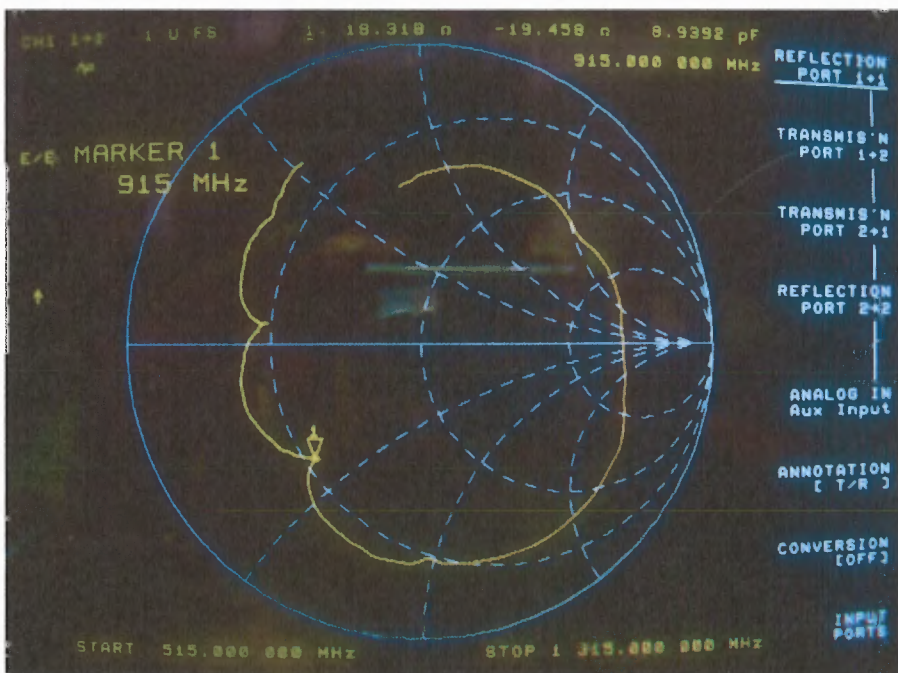


Figure 4.10 Measured Impedance on Smith Chart

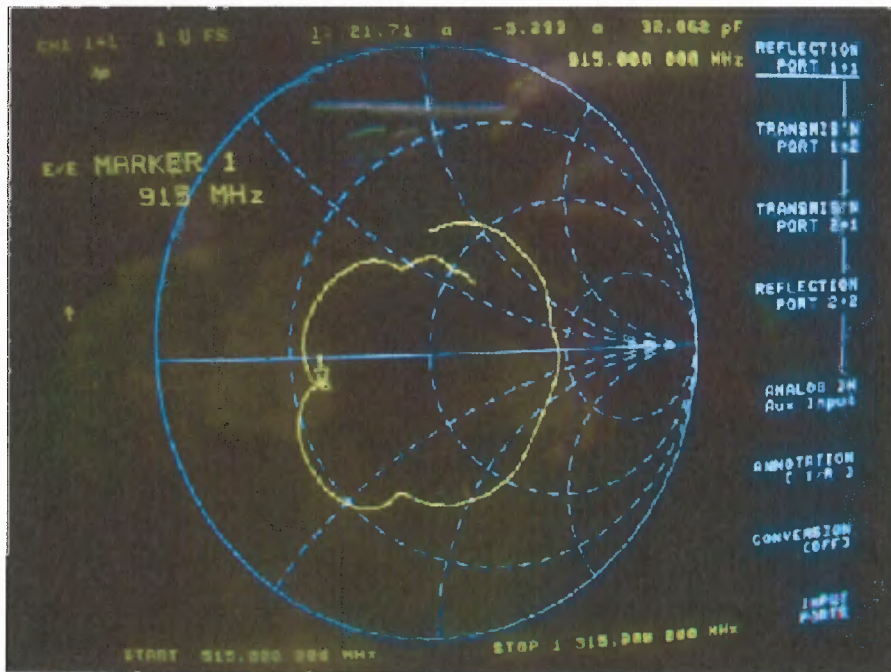


Figure 4.11 Smith Chart of Antenna Model-2 with integrated NIC-Cap(min)



Figure 4.12 Smith Chart of Antenna Model-2 with integrated NIC-Cap(max)

Further experimental work is in progress to include NIC circuitry to antennas mentioned as Model-3 and Model-4.

CHAPTER 5

CONCLUSIONS

The study proposed a new circuitry for Non-Foster matching of antennas which are used as UHF RFID transponder antennas. The improvements presented in this work over previous similar works are Negative Impedance Converter circuitry's low power consumption, low production cost and integration on the proposed antennas' boards resulting in more compact structure.

Also proposed in this study are four different types of printed dipole antennas that have Marchand baluns and capacitively coupled-excitation point. This results in a more suitable structure for chip-excitation which is used in RFID Tags. Additionally, for the Antenna Model-2, a newly proposed structure is designed which includes resonator coupling. This structure is expected, according to simulations made, to help increasing the reading range of the RFID Tag.

After completing numerical design, Printed Circuit Boards of the antennas were modeled in Cadsoft EAGLE Layout Editor environment in compliance with GERBER RS-274x format. The PCBs were produced in the facility of Delta Circuits Inc, Fairfield, NJ and measurements were done at RF/Microwave & Lightwave Engineering Laboratory of NJIT.

APPENDIX A

MOSFET PSPICE MODELS

Si1031R – Vishay P-Channel 20-V (D-S) MOSFET

```
.MODEL QSi1031R PMOS (LEVEL = 3 TOX = 1.7E-8
+ RS = 32E-2 RD = 0 NSUB = 7E15
+ KP = 1.8E-5 UO = 400
+ VMAX = 0 XJ = 5E-7 KAPPA = 2E-3
+ ETA = 1E-4 TPG = -1
+ IS = 0 LD = 0
+ CGSO = 0 CGDO = 0 CGBO = 0
+ NFS = 0.8E12 DELTA = 0.1)
```

Si1032R – Vishay N-Channel 1.5-V (G-S) MOSFET

```
.MODEL Q2SK1958 NMOS (LEVEL = 3 TOX = 1.7E-8
+ XJ = 1.25E-06 LD = 0 WD = 0
+ TPG = -1 RS = 1.43 RD = 1.299
+ RG = 0 NSUB = 2E17 IS = 0
+ UO = 600 KAPPA = 0.5
+ NFS = 0.1E12 THETA = 0.01
+ KP = 2.461E-5 PHI = 0.75 VMAX = 0
+ CGSO = 0 CGDO = 0 CGBO = 0
+ XQC = 1.0 AF = 1 CBD = 0
+ CBS = 0 CJ = 0 CJSW = 0
+ FC = 0.5 JS = 0 KF = 0
+ MJ = 0.5 MJSW = 0.33 PB = 0.8
+ RSH = 0)
```

APPENDIX B

CIRCUIT SIMULATION SOFTWARE

Advanced Design System 2004A, Agilent:

Advanced Design System (ADS) is a powerful electronic design automation software system. It offers complete design integration to designers of products such as cellular and portable phones, pagers, wireless networks, radar and satellite communications systems, and high-speed digital serial links.

Advanced Design System is the industry leader in high-frequency design. It supports system and RF design engineers developing all types of RF designs, from simple to the most complex, from RF/microwave modules to integrated MMICs for communications and aerospace/defense applications.

With a complete set of simulation technologies ranging from frequency-, time-, numeric and physical domain simulation to electromagnetic field simulation, ADS lets designers fully characterize and optimize designs. The single, integrated design environment provides system, circuit, and electromagnetic simulators, along with schematic capture, layout, and verification capability -- eliminating the stops and starts associated with changing design tools in mid-cycle.

Use ADS and its highly integrated links and support as a basis for your design verification solution. ADS can be used for virtual prototyping, debugging, or as an aid in manufacturing test. To enhance engineering productivity and shorten time-to-market, ADS software offers a high level of design automation and applications intelligence [16].

PSpice 9.1 Student Version, ORCAD:

Cadence® PSpice® A/D is the de-facto industry-standard Spice-based simulator for system design. It simulates complex mixed-signal designs containing both analog and digital parts, and it supports a wide range of simulation models such as IGBTs, pulse width modulators, DACs, and ADCs. Its built-in mathematical functions and behavioral modeling techniques enable fast and accurate simulation of designs with efficient debugging. PSpice A/D also allows users to design and generate simulation models for transformers and DC inductors.

Scalability options include PSpice Advanced Analysis capabilities and integration with MathWorks MATLAB Simulink for co-simulation. Advanced capabilities such as temperature and stress analysis, electro-mechanical simulation, worst-case analysis, Monte Carlo analysis, and curve-fit optimizers help engineers design high-performance circuits that are reliable and withstand parameter variation [17].

APPENDIX C

ELECTROMAGNETIC SIMULATION SOFTWARE TOOLS

Currently available commercial Electromagnetic simulation software packages use different types of Computational Electromagnetics (CEM) methods to solve problems.

These numerical methods are listed below [11]:

- Integral Equation Solvers
 - The Discrete Dipole Approximation (DDA)
 - Method of Moments (MOM) or Boundary Element Method (BEM)
 - Fast Multipole Method (FMM)
 - Partial Element Equivalent Circuit method (PEEC)

- Differential Equation Solvers
 - Finite-Difference Time-Domain (FDTD)
 - Multiresolution Time-Domain (MRTD)
 - Finite Element Method (FEM)
 - Finite Integration Technique (FIT)
 - Pseudo-Spectral Time-Domain (PSTD)
 - Pseudo-Spectral Spatial-Domain (PSSD)
 - Transmission Line Matrix (TLM)

- Other Methods
 - Physical Optics (PO)
 - Uniform Theory of Diffraction (UTD)

Each method has its own advantages and disadvantages. Selection of the method depends on the type of problem which we are trying to solve. In this thesis all antenna 3D modeling and simulation tasks are done by using Ansoft HFSS (High Frequency Structure Simulation) software. This software package uses FEM to solve 3D electromagnetic problems. Therefore, only Finite Element Method is explained below.

Finite Element Method (FEM): The finite element method (FEM) has its origin in the field of structural analysis. Although the earlier mathematical treatment of the method was provided by Courant in 1943, the method was not applied to electromagnetic (EM) problems until 1968. Since then the method has been employed in diverse areas such as wave guide problems, electric machines, semiconductor devices, microstrips, and absorption of EM radiation by biological bodies.

FEM is a more powerful and versatile numerical technique for handling problems involving complex geometries and inhomogeneous media. The finite element analysis of any problem involves basically four steps [**]:

- Discretizing the solution region into a finite number of *subregions* or *elements*,
- Deriving governing equations for a typical element,
- Assembling of all elements in the solution region, and
- Solving the system of equations obtained.

Ansoft High-Frequency Structure Simulation (HFSS) Software

HFSS is the industry-standard software for S-parameter, Full-Wave SPICE™ extraction, and 3D electromagnetic field simulation of high-frequency and high-speed components.

Engineers rely on the accuracy, capacity, and performance of HFSS to design on-chip embedded passives, IC packages, PCB interconnects, antennas, RF/microwave components, and biomedical devices.

HFSS uses FEM to solve EM problems. Featured 3D Full Wave EM Field Simulation capabilities of this software can be listed as follows [15]:

- 3D Full-Wave EM Field Simulation
 - Tangential vector finite elements
 - Adaptive Lanczos Padé Sweep (ALPS) for fast frequency sweeps
 - Inclusion of skin effect, loss, and frequency dependence
 - Pushbutton 3D S-, Y-, and Z-matrix parasitic extraction
 - Automatic adaptive mesh generation and refinement
 - Model healing, automatic feature recognition, mesh resolution control, and fault-tolerant meshing for CAD import
 - Low, medium, and higher-order basis functions
 - Direct and iterative matrix solvers
 - Eigenmode matrix solver
 - Floquet ports
 - Auto-assign for terminal-driven ports
 - Incident field from several sources including small current loop, dipoles, and arbitrary plane waves [13].

APPENDIX D

PRINTED CIRCUIT BOARD DESIGN SOFTWARE

Layout designs and Printed Circuit Board production files of produced antennas of this Thesis, are prepared in compliance with Gerber RS-274X standard and by using Cadsoft EAGLE Layout Editor tool.

GERBER-274X:

- The Gerber Format was originally a subset of EIA RS-274-D. Later the format was then extended by the so called "Mass Parameters" and was then also called RS-274-X.
- On 1980-08-27 the first edition of the GERBER FORMAT, Plot Data Format Reference Book was published by Gerber Systems Corporation as a specification to drive the photoplotter of this company. At this time the photoplotter had a limited set of fixed apertures of different shapes (typically round and rectangular and a few others) in different sizes. An aperture could be exposed at a specific coordinate (flash) or the head was moved with open shutter from one coordinate to another to generate line or circular arc segments.
- Mechanical Gerber plotters used apertures made of photographic film, where the transparent portion could be any shape. Flash apertures in custom shapes were used for surface mount pads or edge connector pads or targets to align the layers. If a circle was used to draw a line, the middle of the line would be exposed to more light than the edges, so a Draw aperture was typically a doughnut shape

with the center dark for uniform coverage. This is no longer necessary with raster plotters.

- There was no uniform position for the film apertures, so an aperture list (plain text) was used to inform the operator where to install the apertures before running the plot. The machine had a certain number of available aperture position numbers that were not consecutive 1..max, and usually not all were used for any given board plot. The person generating the plot file had responsibility to ensure that the aperture list used positions that were actually available and matched the plot file.
- In 1986 the GERBER Format was extended to support apertures with variable sizes to produce rectangles of arbitrary sizes within a given range and tapered lines. This functionality is not in practical use any more.
- On 1991-04-26 with the availability of raster-scan capability the GERBER Format was then again extended for polygon areas and Extended Mass Parameter, allowing to dynamically define apertures of different shape and sized and more.
- The last edition of the GERBER FORMAT, Plot Data Format Reference Book was published on 1993-01-31 by Gerber Systems Corporation.
- Later the Gerber Systems Corporation joined with Barco Graphics, Gent, Belgium, and on 1998-09-21 the RS-274X Format User's Guide was published by the Barco Gerber Systems Corporation.
- Again sometime later the rights on the specification turned over to ManiaBarco GmbH, Germany

- On 2003-01-01 ManiaBarco GmbH, Germany was taken over by MANIA Technologie AG, Germany. Since then no "official" public documentation on the GERBER Format is available.
- Today, the Gerber Scientific Instruments Company, a pioneer in photoplotter manufacturing, and a former division of Gerber Scientific, Inc. is no longer in the business of photoplotter for printed circuit board

Around the year 1990 the GERBER Format was adopted by several other photoplotter vendors and also Computer-aided manufacturing tools for PCBs. It became a de-facto standard even if no official documentation is available.

Cadsoft EAGLE:

EAGLE (Easily Applicable Graphical Layout Editor) is a proprietary ECAD program produced by Cadsoft in Germany (American marketing division: Cadsoft USA). It is very commonly used by private electronics enthusiasts, because there is a very usable free demo version for nonprofit use and is available in English and German. Cadsoft has released versions for Microsoft Windows, Linux, and Mac OS X.

EAGLE provides a schematic editor, for designing circuit diagrams and a tightly integrated PCB layout editor, which automatically starts off with all of the components required by the schematic. Components are manually arranged on the board, with the help of coloured lines showing the eventual connections between pins that are required by the schematic, to aid in finding a placement that will allow the most efficient track layout.

It also provides a good autorouter, which once the components have been placed will attempt to automatically find an optimal track layout to make the electrical connections. It does not always manage to find a way of routing all the signals, although it permits manual routing of critical paths such as power and high frequency lines before letting the autorouter handle the other connections.

The .brd files that EAGLE uses to store board layouts are accepted by many PCB production houses.

EAGLE is very popular with hobbyists because the free demo is able to create usable PCBs. (Free ECADs from some companies are crippled so that they won't save or won't print.) The only limitations of boards made with the EAGLE demo are: 2 copper layers; a maximum size of 80mm x 100mm (½ Eurocard)(~3in x ~4in). The demo version of the schematic editor module can only create single-sheet schematics [16].

REFERENCES

1. Wikipedia.org, *Radio-Frequency Identification*, <http://en.wikipedia.org/wiki/RFID> (last accessed: May 1st, 2009).
2. Marrocco, G. (2008), *The Art of UHF RFID Antenna Design: Impedance-Matching and Size-Reduction Techniques*, IEEE Antennas and Propagation Magazine, Vol. 50, No.1, 1045-9243.
3. Strauss, L. (1970). *Wave Generation and Shaping*, McGraw-Hill, 0070621616.
4. Finkenzeller, K., *RFID Handbook: Radio-Frequency Identification Fundamentals and Applications*, Wiley, 0-471-98851-0.
5. Lahiri, S., *RFID Sourcebook*, Prentice-Hall PTR, 0-13-185137-3.
6. Pozar, D. (2005), *Microwave Engineering – 3rd Edition*, Wiley, 0471448788.
7. Brown et al.(2007), *United States Patent Application Publication – Electronic Enhancement and Decoupling*, US2007/0290941 A1.
8. Aberle, J. T. (2007), *Antennas with Non-Foster Matching Networks*, Morgan & Claypool, 1598291033.
9. Sorrells, P. (2000), *Optimizing Read Range in RFID Systems*, <http://www.edn.com/contents/images/84480.pdf> (last accessed: May 1st, 2009).
10. Wikipedia.org, *Computational electromagnetics*, http://en.wikipedia.org/wiki/Computational_electromagnetics (last accessed: May 1st, 2009).
11. Ionescu, B. C., *A Study of RFID Devices and Efficient Ways of Simulating RFID Systems with Maxwell Software*, http://www.ansoft.com/news/articles/rfid_systems_with_maxwell_software.pdf (last accessed: May 1st, 2009).
12. Sadiku, M. (2001), *Numerical Techniques in Electromagnetics – 2nd Edition*, CRC Press, 0-8493-1395-3.

13. Ansoft Corp. website: <http://www.ansoft.com/products/hf/hfss/new.cfm> (last accessed: May 1st, 2009).
14. Wikipedia.org, *Gerber File*, http://en.wikipedia.org/wiki/Gerber_File (last accessed: May 1st, 2009).
15. Agilent, Corp. website:
<http://www.home.agilent.com/agilent/product.jsp?cc=US&lc=eng&ckey=1297113&nid=-34346.0.00&id=1297113> (last accessed: May 1st, 2009).
16. Orcad Corp., website:
http://www.cadence.com/products/orcad/pspice_simulation/pages/default.aspx (last accessed: May 1st, 2009).
17. Niver, E., K. Mouskos, T.Batz, and P.Dwyer, "Evaluation of the TRANCOM's System for Managing Incidents and Traffic (TRANSMIT)," IEEE Transactions on Intelligent Transportation Systems, vol.1, no.1, pp.15-31, March 2000.
18. Vishay Inc., website: <http://www.vishay.com/docs/71171/si1031r.pdf> (last accessed: May 1st, 2009).
19. Vishay Inc., website: <http://www.vishay.com/docs/71172/si1032r.pdf> (last accessed: May 1st, 2009).
20. Johanson MFG, website: <http://www.johansonmfg.com/pdf/Thin-Trim.pdf> (last accessed: May 1st, 2009).
21. Arnaud-Cormos, D., Letertre, T., Diet, A., Azoulay, A. (2007), *Electromagnetic Environment of RFID Systems*, Proceedings of the 37th European Microwave Conference, 978-2-87487-001-9.